

Master Thesis

CODEN:LUTMDN/(TMMV-5262)/1-54/2014



LUND UNIVERSITY
Lund Institute of Technology

Effects of Cooling Rate and Silicon Content in Al/SiC-MMC

Emma Bengtsson

Mikael Hörndahl

2014

DEPARTMENT OF MECHANICAL ENGINEERING
LUND INSTITUTE OF TECHNOLOGY

Preface

This master thesis was performed at the Division of Production and Materials Engineering at the Faculty of Engineering at Lund University in cooperation with Volvo Car Corporation during the autumn of 2013 and spring 2014, within the project *SiCALight II* financed by Vinnova and Volvo Cars.

Supervisors:

Ph.D. Volodymyr Bushlya at the Division of Production and Materials Engineering. Stefan Kristiansson, Volvo Car Corporation, Floby

Examiner:

Professor Jan-Eric Ståhl at the Division of Production and Materials Engineering.

Special thanks:

We would like to thank our families and friends whom have supported us during this time. Sofie Borre and Jacob Corneliusson for proofreading the report, Zivorad for helping us with the tensile tests, Svante and Ryszard for letting us use their workshop and all the others at the department. We would also like to send an extra big thank to Linda, Magnus, Patrik and Roger for the warm welcome and a wonderful tour at Floby.

And finally an extra warm thank to our supervisors and examiner for answering all our stupid questions!

Abstract

This master thesis is about the microstructural and mechanical properties of metal matrix composites (MMC) based on aluminium – silicon carbide. This project is part of a larger collaboration between Volvo Car Corporation (VCC) and Lund institute of Technology. The scope of the thesis is to investigate the effects of cooling rate and silicon content on the microstructure and the mechanical properties.

This thesis has focused on the practical part of the production of MMC. To study the effects several samples were cast in molds of different temperature to see the effects of the cooling rate and later samples were cast while varying the silicon content.

The conclusion is that the cooling rate has little effect on the properties unless it is taken to the extreme and the effects of the silicon content is no more pronounced than for non-reinforced aluminium.

Overall the matrix properties are well coherent with established theory, almost disregarding the presence of carbides.

Table Of Contents

1	Introduction	1
1.1	Background	1
1.2	Aim	1
1.3	Delimitations	1
1.4	Company description	1
1.5	Production	2
2	Theory	3
2.1	MMC	3
2.2	Silicon carbide	3
2.3	Phase diagram	4
2.4	Solidification during casting	5
2.5	Casting method	6
2.6	Biot-number	6
2.7	Thermocouples	6
2.8	Testing of mechanical properties	7
2.9	Literature survey	8
3	Method	13
3.1	Current material	13
3.2	Part 1 - Cooling rate	14
3.3	Part 2 - Silicon content	16
3.4	Testing	17
4	Results	19
4.1	Current material	19
4.2	Part 1 - Cooling rate	23
4.3	Part 2 - Silicon content	37
5	Conclusions	45
5.1	Discussion	45
5.2	Sources of error	49
5.3	Summary	50
5.4	Topics for future research	51
6	References	53

1 Introduction

1.1 Background

Today most of Volvos brake disks are made from cast-iron, but some models feature brake disks manufactured from an aluminium alloy reinforced with silicon carbide particles, a metal matrix composite. The early tests show some difficulties in the machining of the new material, a problem they believe stems from a combination of the alloy and the casting process.

The problems include a large amount of soft and ductile matrix alloy, a large distribution of the size of silicon carbide particles as well as an uneven dispersion of the hard particles.

1.2 Aim

The scope of this master thesis is to solve the problems associated with the material and the casting process. The project will investigate the mechanical and microstructural properties of different matrix alloy compositions and the effects of the cooling rate in the casting process.

1.3 Delimitations

- No other matrix material than the aluminum alloy chosen by Volvo Cars will be considered, however the alloy constituents will be varied.
- Different types of reinforcing particles will not be examined.
- Machinability will not be investigated.

1.4 Company description

Volvo Cars is one of the world's largest manufacturers of automobiles and have a long history of car production in Sweden. They have always been on the forefront of invention during the company's history. Today they are the first car producer in the world to offer aluminium brakes on mass-produced cars.

1.5 Production

To manufacture the brake disk the alloy is prepared in a melting furnace and mixed with the particles. The brake disks are cast in molds kept at a constant temperature of 350 degrees Celsius. The mold is made from a heat resistant, high-alloy tool steel. After casting the disks are machined in two steps and finally treated in an electro plating process.

2 Theory

2.1 MMC

Metal matrix composites (MMC) are a collection of materials with ceramic particles, whiskers or fibers dispersed in a metal matrix. MMC has greater mechanical properties, high-temperature properties and wear resistance compared to the matrix alloy. Until recently MMC materials has been used mostly in aerospace and military applications, due to the high costs associated with the material. (1 p. 3)

In all composite materials it is desirable to have a matrix of a soft and ductile material. Several materials are suitable but aluminium is often chosen because of its affordable price, low weight and good mechanical properties as an alloy.

For optimum strength in the composite material the carbide particles should be harder than the matrix, within a small size range and evenly distributed in the matrix. (2 p. 624)

Today the matrix alloy used by Volvo consists of 9 wt-% silicon, 0.6 wt-% magnesium and the remainder aluminium. The addition of silicon improves the mechanical properties of the alloy as does the small amount of magnesium, as well as increasing the casting properties of the alloy. The combined effect gives a strong alloy, well suited for casting with good machinability. (3 p. 394)

2.2 Silicon carbide

Silicon carbide (SiC) is a ceramic and is therefore nonreactive with the aluminium alloy at ambient temperature. Moreover, it is a lightweight material, which is advantageous in the brake discs when you want to reduce the rotating mass and to obtain a low unsprung mass of the car. The material is also inexpensive and can handle very high temperatures without its hardness deteriorating.

Table 1: Overview of selected properties in the MMC.

	Matrix(4 p. 59)	SiC(5 p. 421)
Hardness [HV]	85	2100 - 2500
Density [kg/m ³]	2650	1200 (LPD)
Youngs Modulus [GPa]	77	405
Tensile Strength [MPa]	200	410
Thermal Conductivity [W/mK]	165	150
Thermal Expansion [µm/mK]	21	4.4

2.3 Phase diagram

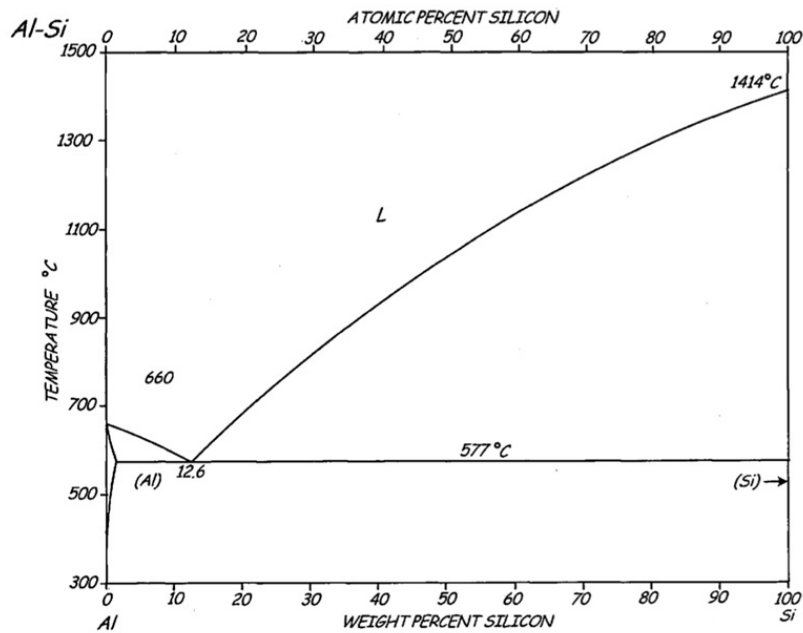


Figure 1: Phase diagram of Al-Si.

The phase diagram shows the different phases of the alloy for different temperatures and different silicon content. The phase diagram however has the disadvantage that it only shows the phases present if the temperature change is very slow, i.e. the diagram is independent of time.

With increasing silicon content up to the eutectic the resulting microstructure becomes more lamellar and the melting interval becomes narrower and solidification begins at a lower temperature. For the eutectic composition the melting interval has disappeared and the resulting microstructure becomes completely lamellar. (6 p. 670)

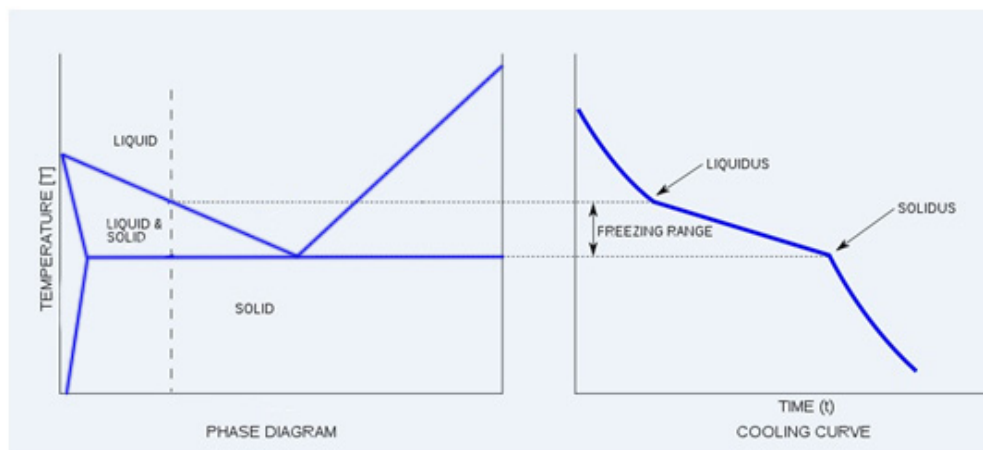


Figure 2: solidification range in alloys.

2.4 Solidification during casting

In casting the molten metal solidifies as a solidification front that travels from the cavity walls towards the center of the casting. (6 s. 583)

For any alloy, containing two or more alloying elements, during cooling there is a primary dendritic forming under the liquidus temperature and a eutectic structure forming during the later phase of solidification. During solidification the chaotic structure of the melt transforms into the ordered structure of the solid. This transformation can have different appearance depending on the rate of cooling. (7 pp. 37-39) Different cooling rates produce different microstructures and properties of the finished product. A faster solidification results in smaller grains and a harder, more brittle material; whereas a slow cooling gives the grains sufficient time to grow and produce a ductile material with large grains. (4 p. 241)(8)

For eutectic compositions the solidification of both phases present takes place at the same time. In the case of normal eutectic growth both phases grow at the same speed and form a characteristic eutectic structure, usually lamellar. The lamellar distance and the solidification rate is determined by the degree of undercooling of the melt, as well as thermodynamic and kinetic factors. (7 p. 40)

It can also be observed that primary α -grains surrounded by eutectic mixture of α and β and that SiC particles is pushed by primary α -phase into the last solidification regions, i.e. the grain boundaries. The SiC particles also work as a barrier preventing grain growth. This fact explains the decrease in average grain size with increasing in amounts of SiC. (9)

During solidification the metal emits a certain amount of energy, known as the heat of fusion. As a liquid, the energy is bound in the material to give the atoms the extra level of movement. To melt the material this energy has to be supplied to facilitate the phase change from solid to liquid. (2 p. 402)

In the production of cast material the casting process chosen will have a major impact on the material properties. To improve and optimize the properties of materials it is important to take into account how the process can dissipate heat from the melt, these are; metallurgical treatment, alloy composition and solidification manner.

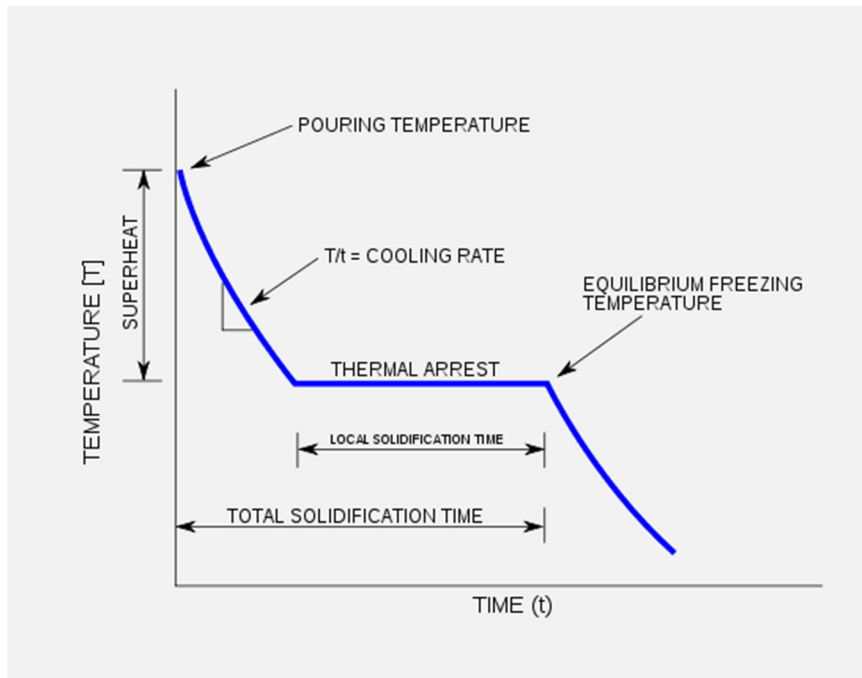


Figure 3: Example of a cooling curve.

2.5 Casting method

During up-hill casting the mold cavity is filled with the melt from the bottom up. This has many advantages for the end result, better surface finish and less surface cracking, compared to conventional casting where the melt is added from the top. (3 p. 257)(10) Volvo is using a variant of up-hill casting where they apply pressure to the part during solidification, this technique is called squeeze casting.

2.6 Biot-number

The biot number is a dimensionless factor indicating the relationship between the heat transfer into or away from a body compared to the temperature gradient inside the body. The biot number is calculated with Equation 1, where h is the heat transfer coefficient, x is the characteristic length of the body and k is the thermal conductivity of the body. (11 p. 236)

Equation 1

$$Bi = \frac{h * x}{k}$$

If the biot number is <0.1 the temperature gradient in the body can be neglected as the temperature difference within the body will be less than 5%.(12)

2.7 Thermocouples

In 1821 Thomas Seebeck discovered the thermoelectric effect, where two wires of dissimilar metals connected at both ends and one of the ends is heated, there flows a continuous current through the wires. This effect is used for thermal measurements in thermocouples, by measuring the voltage produced in the wires. (13 pp. z-21)

2.8 Testing of mechanical properties

There are several methods to test the mechanical properties of a new material, the ones used in this project is tensile testing of machined rods and hardness testing of cut pieces from the cast samples.

2.8.1 Tensile testing

To evaluate a material's properties and behavior under tension a tensile test can be performed. A rod machined to close tolerances is placed in a testing rig and pulled with a constant velocity meanwhile the elongation and the pulling force is measured. The data can then be plotted in a stress-strain diagram.

Information about the mechanical properties of the material can be obtained from the data, such as the yield and tensile strength, the Young's modulus as well as the elongation at breakage. (4 pp. 57-62)

2.8.2 Indentation hardness

Another way to measure a materials resistance to deformation is to measure its hardness. This is done by applying force to a small, hard indenting body. The magnitude of the force and the shape of the indenting body are determined in accordance with a standard. The resulted deformation is a measurement of the relative hardness of the material. Indentation hardness can be classified according to the size or the depth of the impression left by the measurement. The three major categories are macro-, micro- and nanoindentation.

For this project macro indentation according to Rockwell B standard will be used to compare the results. The standard specifies the indenting body as a steel sphere with 1.588 mm diameter (1/16"). The force shall be 100 kilogram force. (4 pp. 68-73)

2.8.3 Scanning Electron Microscope (SEM)

A scanning electron microscope (SEM) is a type of microscope that uses electrons to scan the sample surface. The sample is placed in a vacuum chamber since the atoms in the air would scatter the electrons. An electron beam is moved over the sample surface in a raster pattern and information from the sample is gathered from the interaction between the electrons in the scanning beam and the electrons in the sample. The information is collected either via a backscatter detector or a secondary electron detector. To determine the topography of the sample a secondary electron detector can be used, while the backscatter electron detector is used to determine the average atomic number in different points in the sample. The resulting image is based on the information from the detected signal combined with the position of the electron beam. (14 pp. 187-190)

2.8.4 Energy Dispersive Spectroscopy (EDS)

Energy dispersive spectroscopy (EDS) is a technique for analyzing materials using x-rays or high-energy particles (e.g. electrons or protons) to excite the sample material and examine the resulting radiating energy levels. This process works because each element has a unique atomic structure and a set of characteristic peaks in its x-ray spectrum. (14 p. 196)

2.9 Literature survey

As this project is part of a large project about the preparation and subsequent processing of metal matrix composites, a literature survey about forging and high pressure die casting of these alloys has been include.

2.9.1 Forging

In a test conducted by Joardaret. al. (15) it has been found that the carbide content has a large influence on the mechanical properties of the material and the result during forging. For example the yield and tensile stresses of the material increase while the ductility decrease with increasing carbide content or when the particle size of the reinforcement is decreased. It has also been observed that the hardness and compressive strength increase with higher carbide content, as can be seen in Figure 4.

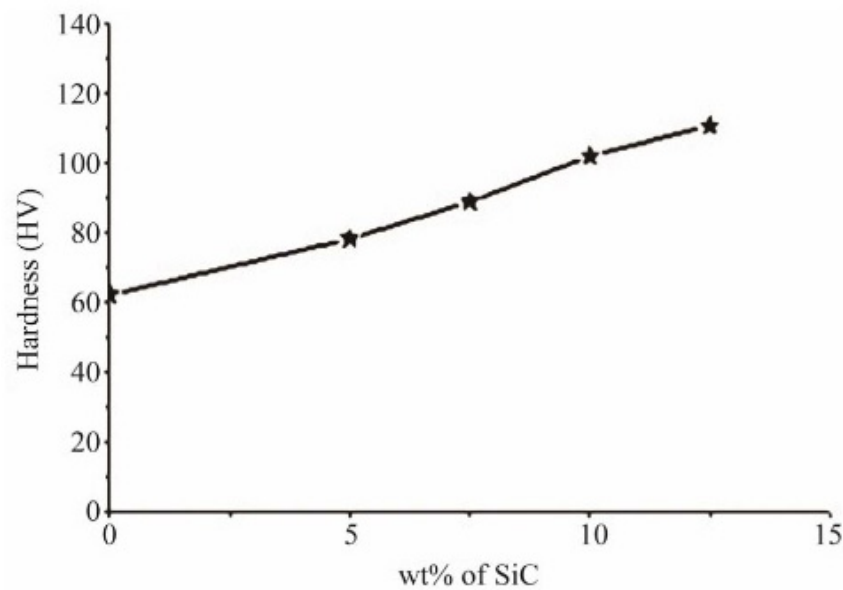


Figure 4: Variation in hardness with carbide content.

The observed increase is believed to be caused by the difference in the plastic and the elastic behavior of the matrix versus the particles. Another theory is that the increased carbide content causes smaller grains in the matrix alloy, which in turn could explain the improved performance.

During testing two types of crack formation were found; speed cracks, and surface cracks. Surface cracks occur when surface temperature exceeds the lowest melting temperature of the present phases. Primary cause is a conversion from compression work to thermal energy. Speed cracks are caused by excessive stresses caused by barreling during deformation. Cracks began forming after 28% – 32% height reduction, highly dependent on the carbide content. Complete collapse was achieved after 34% – 38% reduction in height.

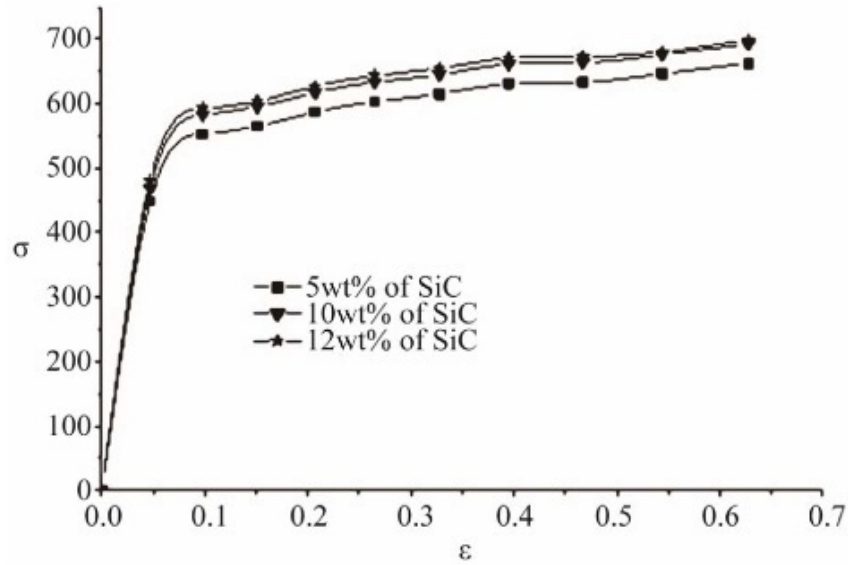


Figure 5: Variation of equatorial stress during forging.

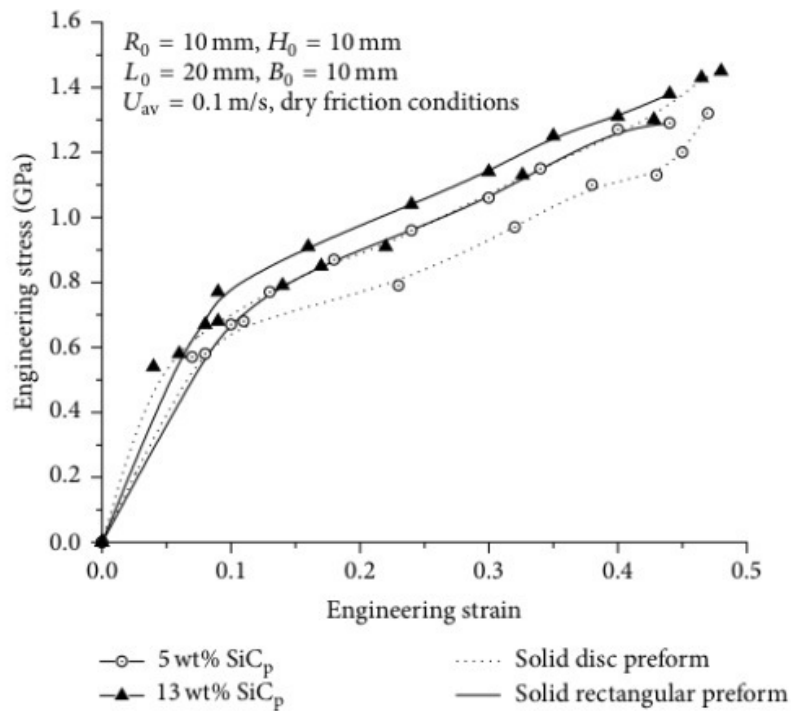


Figure 6: Experimental variation of stress with strain.

Another study, performed by Deep Verma et al in 2013 (16), determined that the maximum deformation was 47% – 49% with maximum stresses reaching 1.5 GPa at room temperature. In general the stresses required for the same strain increased with higher amount particles, meaning a greater force to achieve the same deformation. It was also concluded that the shape of the sample had an effect, with the rectangular preforms showing larger stresses due to the sharp corners.

Overall the results show a decrease in forgeability with increased carbide content, as these samples require higher forging forces and have a higher tendency for equatorial cracks during deformation.

A study conducted regarding the microstructure of forged samples (17), showed that forged samples had a uniform carbide distribution for a large span of carbide compositions. The study also investigated the fatigue strength for forged samples contra cast. For low carbide content, up to 5 wt%, there was a significant increase in fatigue strength compared to cast samples. For medium particle content, 7.5% – 10%, there was no observable increase. The fracture damage was mainly due to failed bonding between particles and matrix.

2.9.2 High pressure die casting (HPDC)

Castability of aluminium alloys varies with composition. The easiest alloy to cast is one of aluminium-silicon since it provides the greatest fluidity for casting of deep, thin section. Generally, higher silicon content up to the eutectic (about 12,5%), provides an easier alloy to cast.(18)

The castability of an alloy is also dependent of the amount of reinforced particles, e.g. 15wt% SiC proved extremely difficult to cast due to wall adhesion in the die. (9)

It is important to minimize chemical reactions between the matrix and the particles during processing, to produce a material with homogenous distribution of reinforced particles and to minimize microstructural defects. Also, the mixing parameters of SiC were critically important to achieve good quality of the composite structures. To achieve a good load transfer across particle-matrix boundary it is important to achieve a good wetting of the carbides.(9)(19)

A number of parameters have shown to be of importance for the optimization of this process. The temperature of the molten metal before introducing SiC, and the casting temperature are two of the parameters which should be controlled. For the machine, the most important parameters are speed and pressure of the plunger, as well as die temperature.(19)(20 pp. 41-43)

Investigation of the microstructure after pressure die casting shows a homogenous distribution of SiC. The microstructure of the matrix is typical of the HPDC structure with a bimodal grain size distribution. As the distance from the surface increases, the average grain size is increased. The average grain size of the matrix is though decreasing with increasing percentage of SiC.

It can be seen that with an increase in the amount of reinforcing particles the microstructure becomes finer. The particles work as nucleation sites during solidification which leads to finer grain size. Particles also act like a barrier which hinders the grain to grow too large. But an increase in porosity could be seen with increasing percentage of SiC particles, possibly resulting from the mixing and gases trapped in the particle clusters. Tensile yield strength increases with addition of SiC, while ultimate tensile strength and elongation decreased. The addition of reinforcement also increases the hardness level. An increase in reinforcement also increases the corrosion rate. It is mainly attributed to the micro-galvanic effect between the SiC particles and the alloy matrix. The corrosion resistance is also affected by the porosity that is enhanced by the presence of SiC particles.(21)(22)

Table 2: Mechanical properties of HPDC material(21).

Property	Al-Si7-Mg0.3-T6	Al-Si7-Mg0.3-T6/β-SiC-15wt%
Ultimate strength (MPa)	220	380
Yield strength (MPa)	180	345
Elongation percentage (%)	18	10
Hardness (HB)	110	130

3 Method

3.1 Current material

3.1.1 Composition

The brake disks manufactured by Volvo Car Corporation today is composed of a matrix of aluminium with; silicon, magnesium, and particle reinforcement. The amount of reinforcement particles is 21 wt% SiC. A wetting agent is used to aid the inclusion of particles. The ingredients in the finished material are shown in Table 3.

Table 3: Ingredients of the melt.

Component	% of total
Aluminium	67,5%
Silicon	9,0%
Wetting agent	1,9%
Other	0,6%
SiC	21,0%

3.1.2 Analyze

To analyze the carbide content several images were taken in a SEM and analyzed with Leica QWin. The images were taken at random places in two different brake disks machined in Floby. Each disk was analyzed in four places, diametrically opposite along the perimeter.

As a future comparison with the tests done during this project the hardness was tested on three different factory produced brake disks. The result of which is shown in Figure 11. Two of these were taken directly after machining and the third had also passed through the electro plating process.

As a final baseline for future experiments a brake disk chosen at random was machined into three test rods for tensile testing and tested to determine the mechanical properties of the material.

One part of the project was to determine the cooling rate of the current production line at Volvos factory in Floby, to use as a comparison to the results from this project. To do this several attempts were made to insert a thermocouple inside the mold cavity, between the two halves of the mold, and have it enclosed by the liquid filling the cavity. The thermocouples chosen for this had a wire diameter of 0.254 mm (0,010") and a diameter with insulation of 0.8 mm. Unfortunately all attempts were unsuccessful due to the close tolerances of the mold in combination with the pressure applied during solidification.

The microstructure of the factory made brake disks were studied to serve as a baseline for the experiments, and to serve as a comparison to the result from this project.

3.2 Part 1 - Cooling rate

3.2.1 Thermal analysis

At the beginning of the project a simplified thermal analysis was conducted. Assumptions were made that the mold and melt was in a closed adiabatic system, and given enough time for the temperature difference to be eliminated. The inserted energy was assumed to be the thermal energies of melt and mold and the heat of fusion of the melt. The resulting temperature was calculated for a body with the thermal capacity of the combined material as shown in Equation2.

Equation2

$$T = \frac{(T_{melt} * C_{p,Al} + \frac{E_{Al}}{M_{Al}}) * m_{melt} + T_{mold} * C_{p,Cu} * m_{mold}}{C_{p,Al} * m_{melt} + C_{p,Cu} * m_{mold}}$$

3.2.2 Sample preparation

To vary the cooling rate of the composite samples they were cast in molds at different temperatures. The temperatures chosen for the experiment were room temperature as a lower extreme, 250°C, 350°C, 450°C and 750°C as the upper extreme. Volvo is casting today in molds at 350°C, this temperature was therefore chosen as the reference with the temperature adjusted a hundred degrees up and down and complemented with two extreme cases.

The molds for the samples have been made from solid copper blocks, circa 3,5 kg a piece. The mold cavity has the shape of a cylinder with diameter 25 millimeters and a height of 125 millimeters. The bottom of the molds were plate machined from austenitic stainless steel, this was to obtain the same linear thermal expansion as the copper and to minimize the cooling rate at the bottom and ideally have a more uniform cooling of the entire sample. The molds are pictured in Figure 7.

The samples for casting have been prepared in a top loaded furnace set at 775 degrees Celsius in a crucible of graphite clay. Most of the materials used in the testing are from recycled brake disks from Volvos production facility in Floby. After a complete melting of the matrix alloy the melt have been agitated with a graphite paddle at 60 rpm for at least 10 minutes.

The samples have all been cast using gravity casting without shielding gas. To aid the casting a stainless steel funnel heated to 750 degrees Celsius was used to center the liquid in the mold. The pouring time was roughly one to two seconds.

To monitor the temperature gradient during solidification a thermocouple was placed in the mold, about five millimeters from the cavity wall and one placed in the center of the mold cavity to be encased in the solidifying metal.



Figure 7: The copper mold used to change the cooling rate.

For the higher mold temperatures, if the molds required a long time to be brought back to the correct temperature after the first casting, the usual procedure was to take the melt out and let it solidify while the molds were in the oven the second time. The melt was later reheated and agitated again for the final casting.

3.3 Part 2 - Silicon content

The silicon content was adjusted to investigate the effects on the matrix material. This was achieved by adding either aluminium with lower silicon content or pure silicon to the desired silicon content. The AA 5083 aluminium alloy used to change the composition has the nominal chemical analysis shown in Table 4. Also magnesium, wetting agents and silicon carbide was added to obtain the same composition as the baseline apart from the silicon content.

Table 4: Chemical composition of AA 5083.

Component	Wt. %	Component	Wt. %	Component	Wt. %
Al	92.4 - 95.6	Si	Max 0.4	Cu	Max 0.1
Cr	0.05 - 0.25	Fe	Max 0.4	Other, each	Max 0.05
Mg	4 - 4.9	Ti	Max 0.15	Other, total	Max 0.15
Mn	0.4 - 1	Zn	Max 0.25		

For the second part of the project new molds were manufactured, this time from medium alloy steel, using the same internal dimensions for the cast samples. One of the molds is pictured in Figure 8. New molds were made to further simulate the current conditions at the Volvo production facility. The samples were cast using the same technique as described previously, in molds at 320 degrees.



Figure 8: One of the steel molds used in the experiment.

To prepare the melt, first brake disks were melted in the furnace, to that the other ingredients were added to change the composition. The carbide particles were added using nitrogen gas through a Sialon tube to the bottom of the crucible during the stirring action of the graphite paddle. A schematic view of the preparation setup is shown in Figure 9. This process is a very slow method of adding carbide particles, at roughly 20 grams per hour. At several times during this process the melt was left to rest without stirring for 30 minutes to aid the inclusion of particles and to reheat the melt to the set temperature. This process was also combined with a large scale, manual stirring operation to equalize the carbide content of the entire mold.

The different matrix compositions tested are with 7, 9, 11 and 12,5% silicon by weight. Today the alloy used by Volvo contains 9 % silicon, therefore this was the reference. From this the percentage silicon was adjusted with two percentage points up and down to see the change. As a final comparison, the eutectic composition (12,5 wt%) was tested.

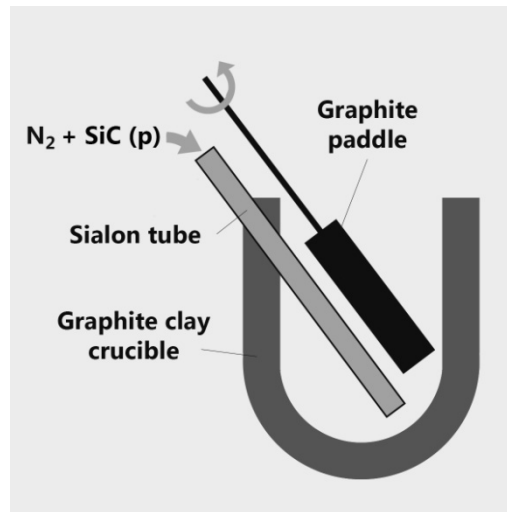


Figure 9: a schematic view of the carbide infusion technique.

3.4 Testing

The samples from both parts were tested for hardness, tensile strength and examined in an optical and a SEM microscope to determine its microstructure as well as carbide content and distribution.

3.4.1 Hardness

The samples were tested for hardness with a hardness tester according to the Rockwell B-standard in ten different locations, well distributed over the cross section of the cast sample.

3.4.2 Tensile test

For tensile testing, rods from all the samples were machined into the dimensions of Figure 10. This was done in a turning operation in a CNC lathe. For machining a diamond insert was used. The rods were tested in a tensile testing rig with a set pull of 2mm/min. The extension of the samples was logged using an extensometer.

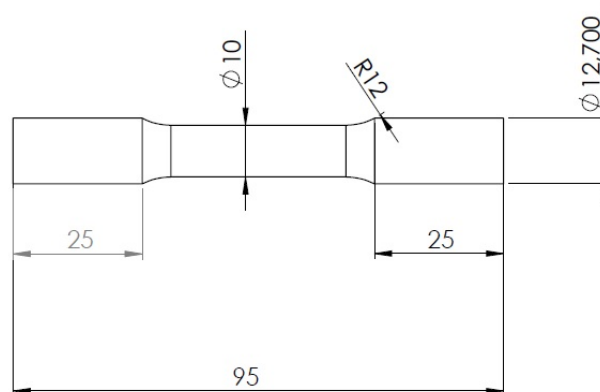


Figure 10: dimensions for the tensile testing rods.

3.4.3 Microscopy

To study the microstructure all samples were prepared in the same way. They were cut using a diamond cutting disk with generous amounts of cooling water. First step in preparing the samples was 500 grit sandpaper, followed by 1200. Second step was polishing with synthetic diamonds in a solution; first with 9 micron and then 1-micron diamond abrasives. The final step was a colloidal solution with silicon oxide. All samples were etched with 10% sodium hydroxide.

3.4.4 Carbide content

To analyze the carbide content the samples were photographed in a scanning electron microscope and the images sent to a computer. The images from the samples were analyzed using Leica QWin for carbide content. The results were given as percentage area. This had to be converted to percentage mass for it to be used as a comparison to the theoretical carbide content used by Volvo during preparation. Equation 3 was used to convert the results. The density for solid silicon carbide was assumed to be 3.21 kg/dm³. (5 p. 415)

Equation 3

$$\begin{aligned}\%_{mass} &= \%_{area} * \frac{\rho_{SiC}}{(\%_{SiC} * \rho_{SiC} + (1 - \%_{SiC}) * \rho_{Al})} \\ &= \%_{area} * \frac{3.21}{(0.21 * 3.21 + (1 - 0.21) * 2.65)}\end{aligned}$$

Which can be simplified to:

$$\%_{mass} = \%_{area} * 1.1598$$

4 Results

4.1 Current material

4.1.1 Hardness

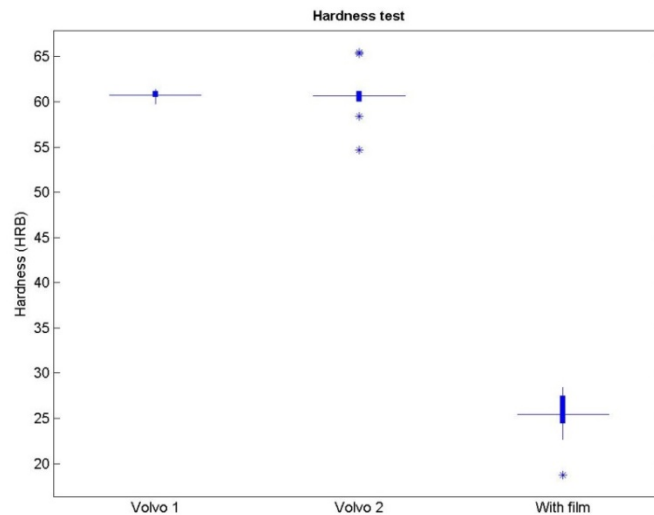


Figure 11: Hardness of brake disks manufactured by Volvo.

4.1.2 Tensile testing

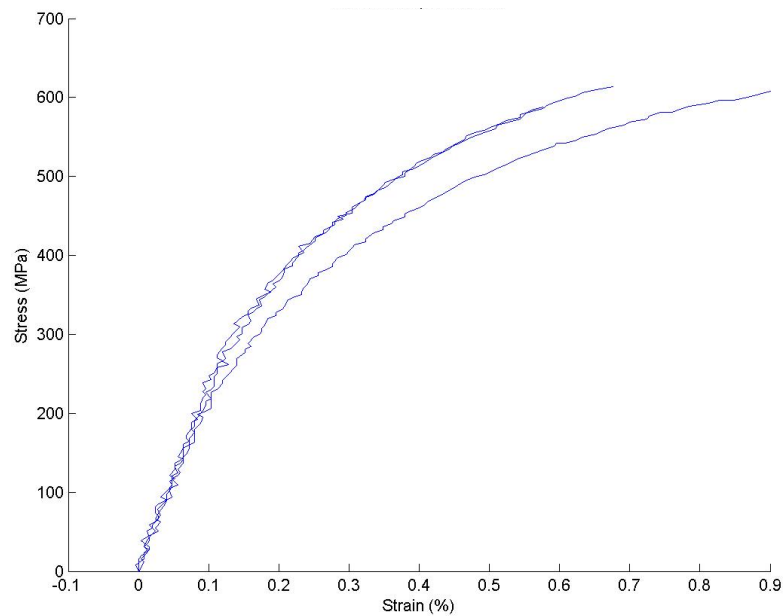


Figure 12: Result of the tensile tests from machined brake disks.

4.1.3 Microstructure

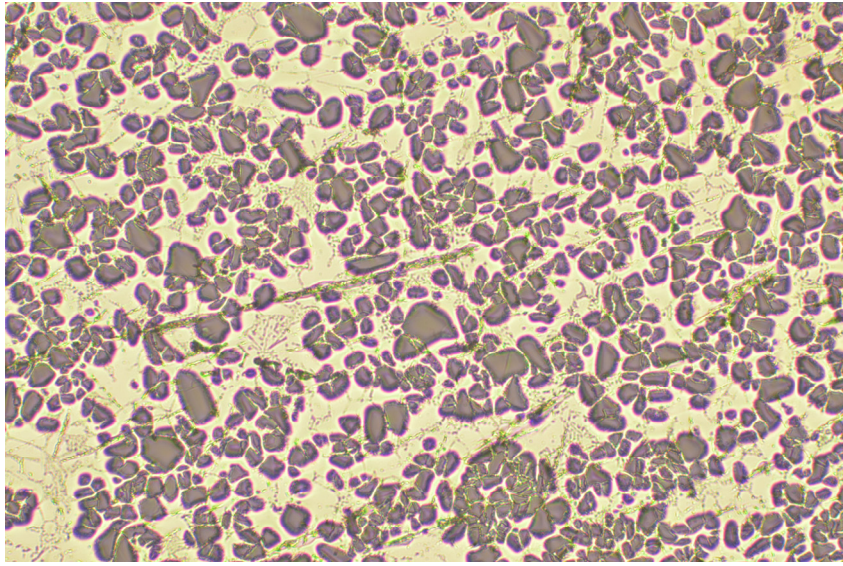


Figure 13; Optical microscope image of brake disk, 100x.

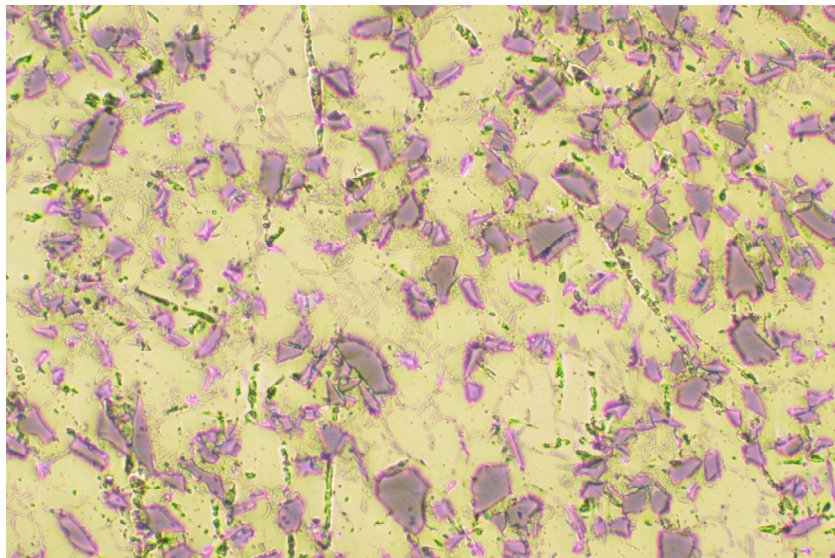


Figure 14; Optical microscope image of brake disk, 200x.

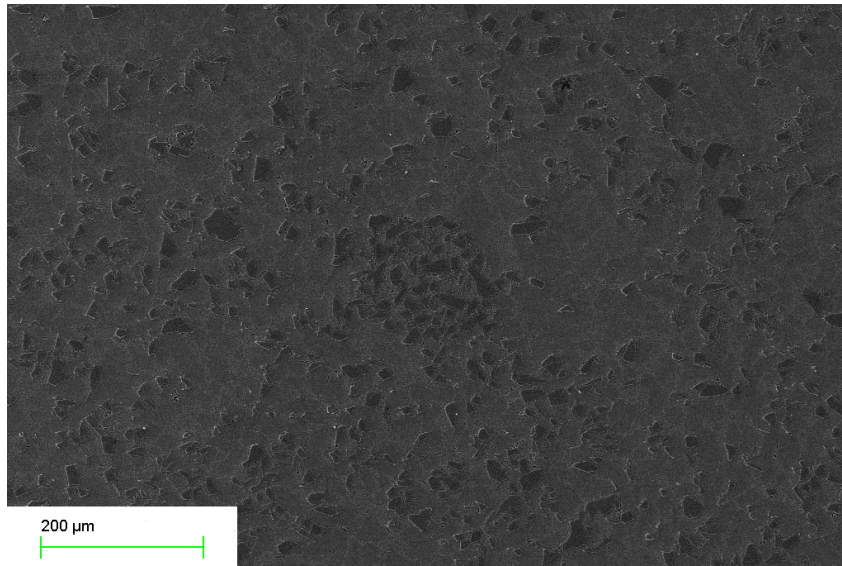


Figure 15; SEM image of brake disk, 280x.

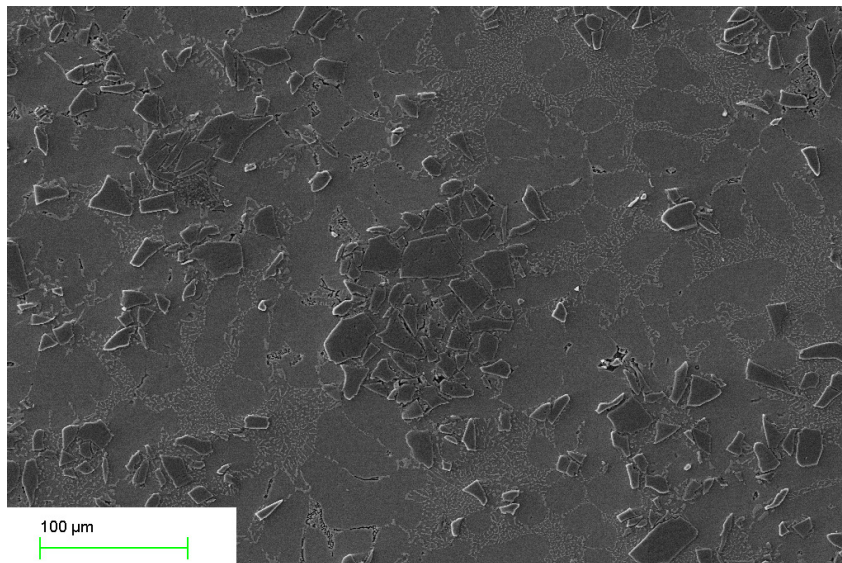


Figure 16; SEM image of brake disk, 500x.

4.1.4 Carbide content

The results from the analysis of carbide content at different test locations as well as the overall average can be seen in Table 5.

Table 5: Analysis of carbide content.

% area	% mass
25,6	29,7
25,1	29,1
22	25,5
12,7	14,7
14,8	17,2
22,7	26,3
21,5	24,9
15,3	17,7
17,1	19,8
18,5	21,5
16,3	18,9
AVG	22,3

4.2 Part 1 - Cooling rate

4.2.1 Thermal analysis

The biot number was calculated with Equation 1 and the data presented in Table 6.

Table 6: Data for calculation of the biot-number.

Length [m]	0,125
Heat transfer coefficient, solid to air	4-12
Thermal conductivity [w/m K]	385

The biot number was calculated as 0.00375, which means that any temperature gradient in the copper molds can be neglected. Thermal analysis with Equation 2 and the data presented in Table 7 (11 p. 418) indicates that the thermal equilibrium for the adiabatic system is at 376 degrees Celsius.

Table 7: Data for the thermal analysis.

$C_{p,Al}$ [kJ/g C]	0,92
$C_{p,Cu}$ [kJ/g C]	0,385
m_{mold} [gram]	5000
m_{melt} [gram]	155
E_{Al} [kJ/mol]	10,71
M_{Al} [g/mol]	26,98
T_{mold} [C]	350
T_{melt} [C]	750

4.2.2 Cooling rate

In the following pages, the results from the temperature measurements are presented. The blue line in all graphs denotes the temperature measured in the solidifying metal. The other colors is one for each mold. By comparing the result for different molds, it is possible to ensure a uniform cooling of all samples.

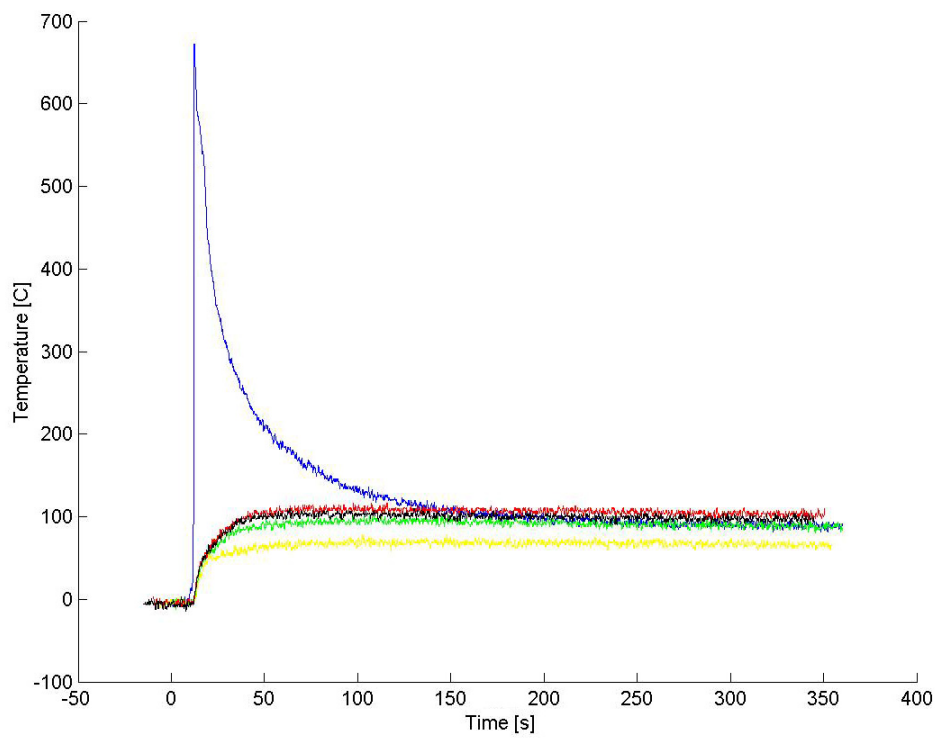


Figure 17: temperature curves from samples cast in molds at room temperature.

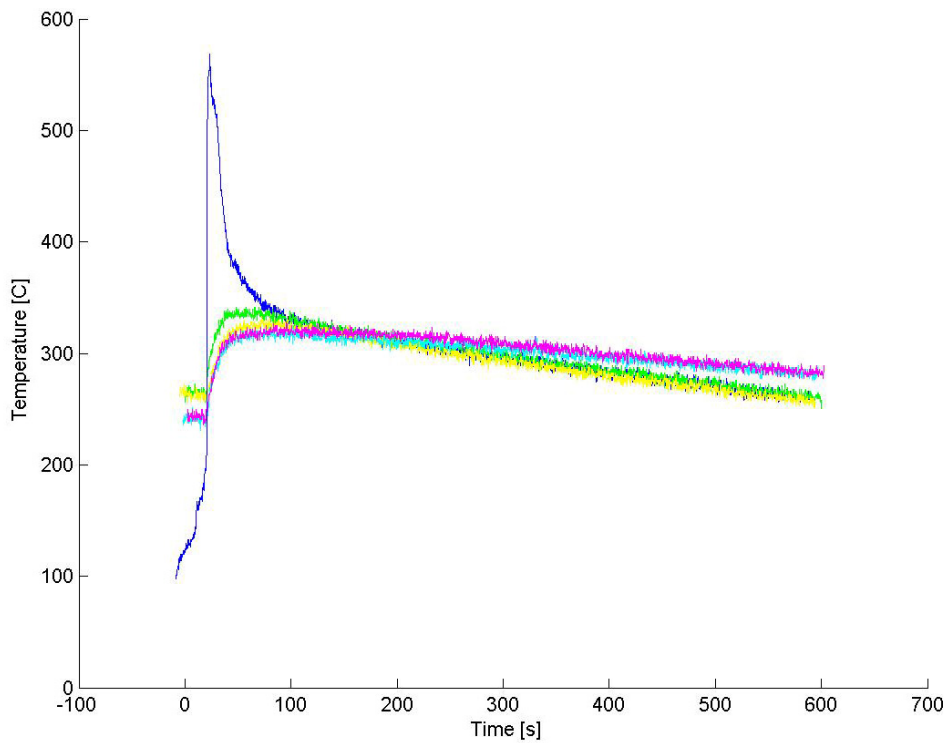


Figure 18: temperature curves from samples cast in molds at 250°C.

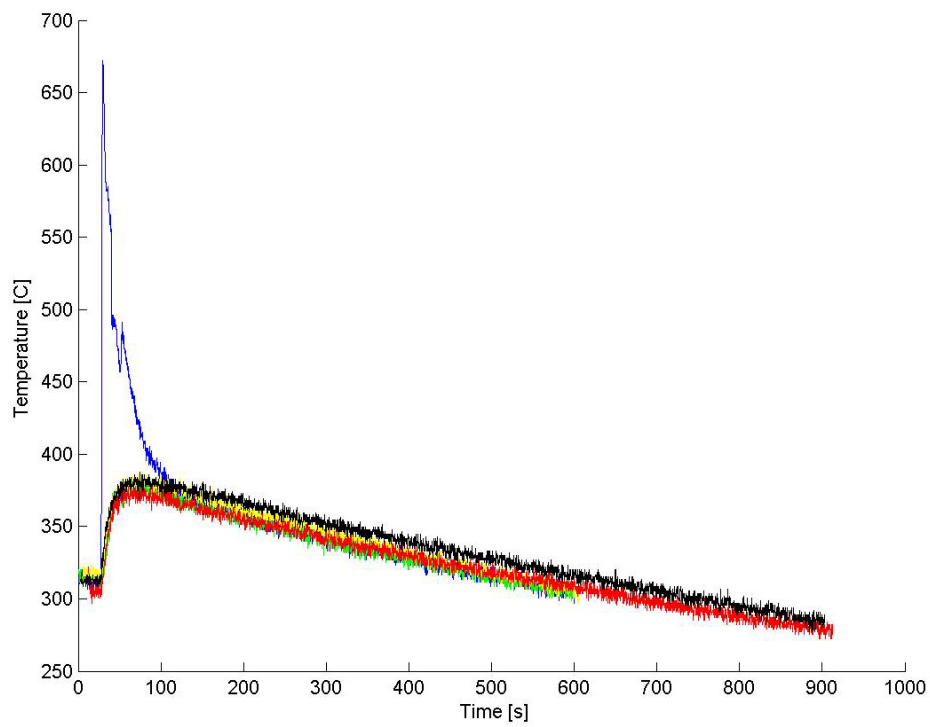


Figure 19: temperature curves form samples cast in molds at 350°C.

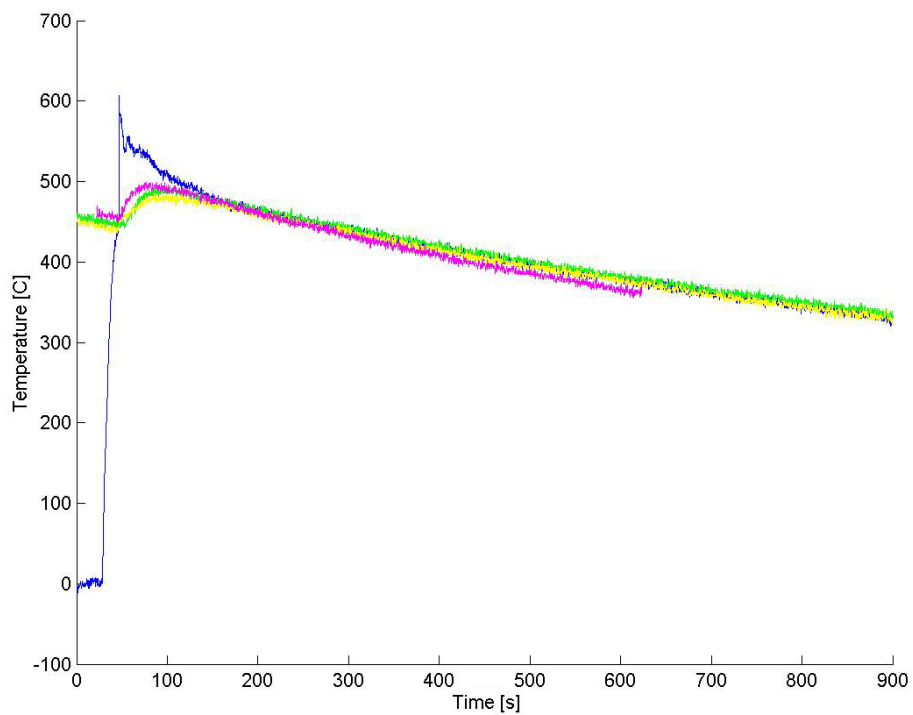


Figure 20: temperature curves form samples cast in molds at 450°C.

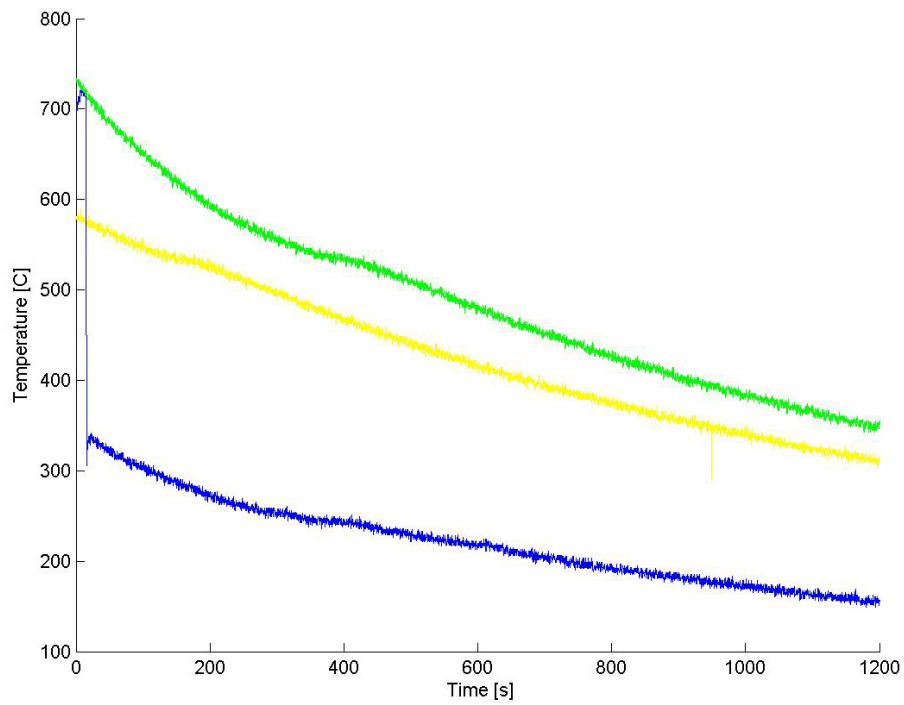


Figure 21: temperature curves form samples cast in molds at 750°C.

For the sample cast in mold at 750 degrees, Figure 21, there is an anomaly in the temperature measurement. This is due to the heat radiating from the mold degrading the insulation of the thermocouple, weakening it sufficiently to be burned away by the rising liquid. From the moment of casting, the temperature actually measured is at the top surface of the rod.

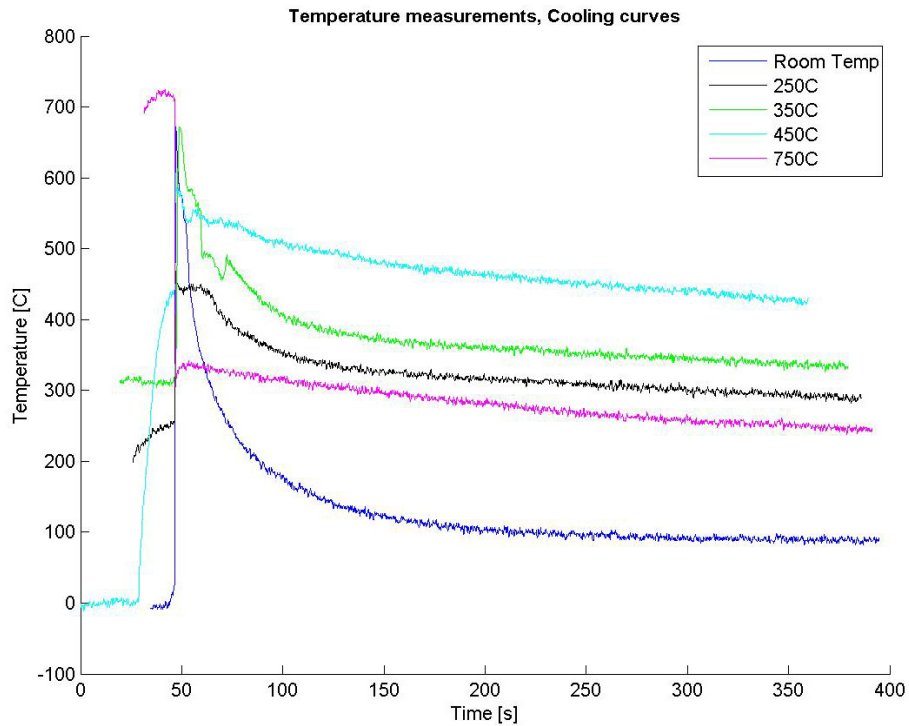


Figure 22: a comparison between the temperature curves for the different samples.

Figure 22 shows a comparison between the cooling curves for the different samples. From this the solidification and recrystallization times can be deduced, shown in Table 8: solidification and recrystallization times for the cast samples Table 8. The temperature range denotes the interval at which solidification is occurring and the recrystallization time is calculated as additional time above 461°C after complete solidification.

Table 8: solidification and recrystallization times for the cast samples.

Sample	Solidification time [s]	Temp range [C]	recrystallization time [s]
Room Temp	2,9	591-540	2,1
250°C	13,5	540-512	3,2
350°C	18,9	583-491	19,2
450°C	16,6	578-555	109
750°C	80,4	542-525	162

4.2.3 Microstructure

4.2.3.1 Molds at room temperature

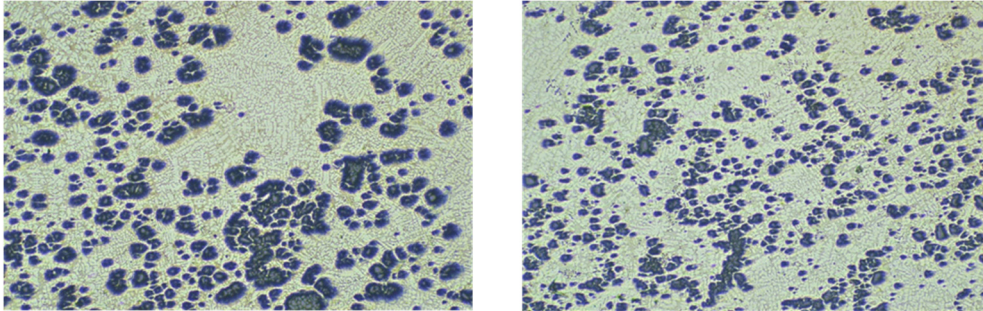


Figure 23; 50x.

To vary the cooling rate of the melt the mold temperatures have been varied. In this case the molds are at room temperature when casting. The structure is a typical cast structure with fine dendrites. The black particles in Figure 23 are silicon carbide and the matrix is gray with a hint of brown. The lighter parts of the matrix are α -phase and between the dendrites is eutectic structure of aluminium and silicon.

Figure 23 shows the distribution of SiC particles in two different locations and Figure 24 shows the matrix structure with dendrites.

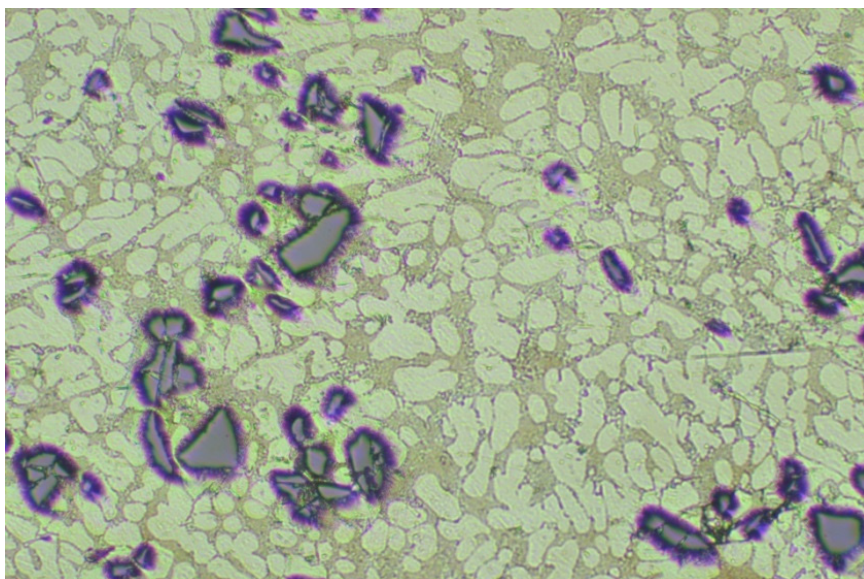


Figure 24; 200x.

4.2.3.2 *Molds at 250 degrees*

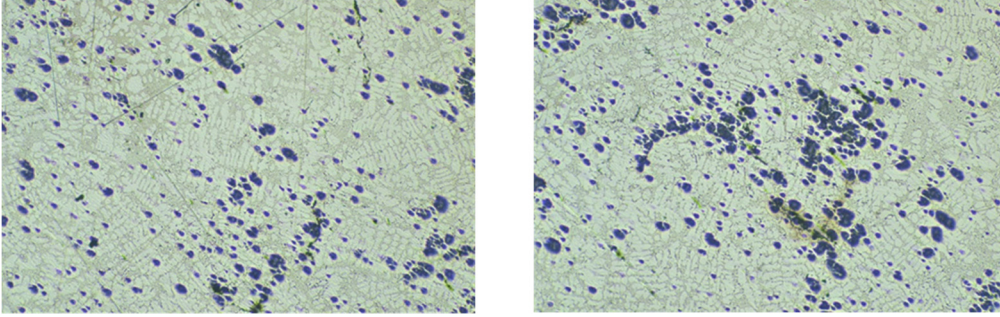


Figure 25; 50x.

To get a slower cooling rate of the melt the mold temperature has been increased to 250 degrees before casting.

As can be seen in Figure 25 the samples have less carbide particles than in the experiment with room-tempered molds. The distribution of particles is also inferior to the earlier experiment. The cast structure shown in Figure 26 is similar to the room tempered experiment.

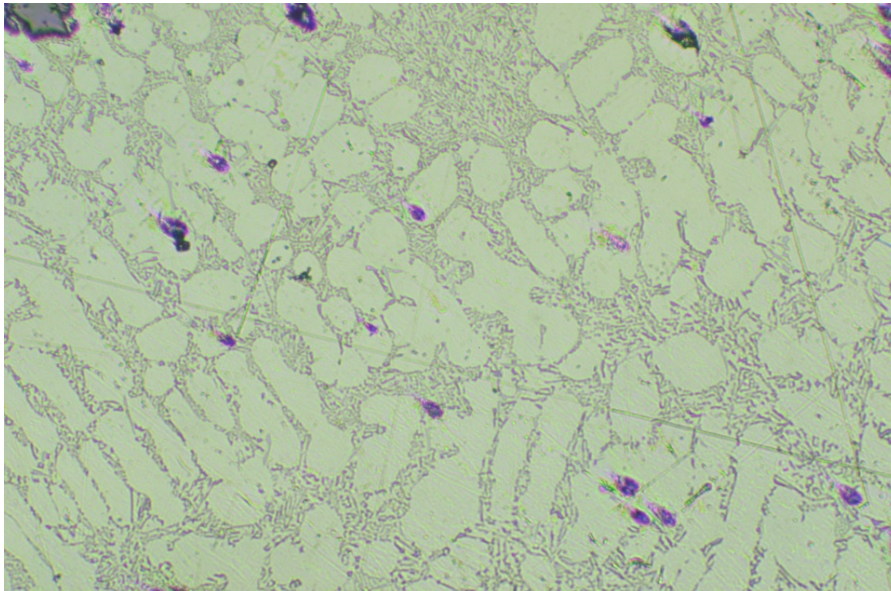


Figure 26; 200x.

4.2.3.3 Molds at 350 degrees

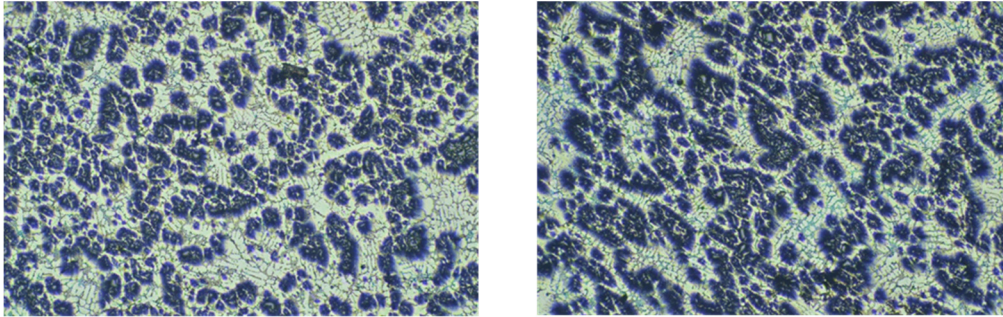


Figure 27; 50x.

To slow down the cooling rate even further the mold temperature has been raised to 350 degrees.

Figure 27 shows the distribution of SiC particles and as it can be seen it contains a lot of carbides. Figure 28 shows the structure of the matrix. It is a more coarse structure compared to the cooler molds since the dendrites have had time to grow.

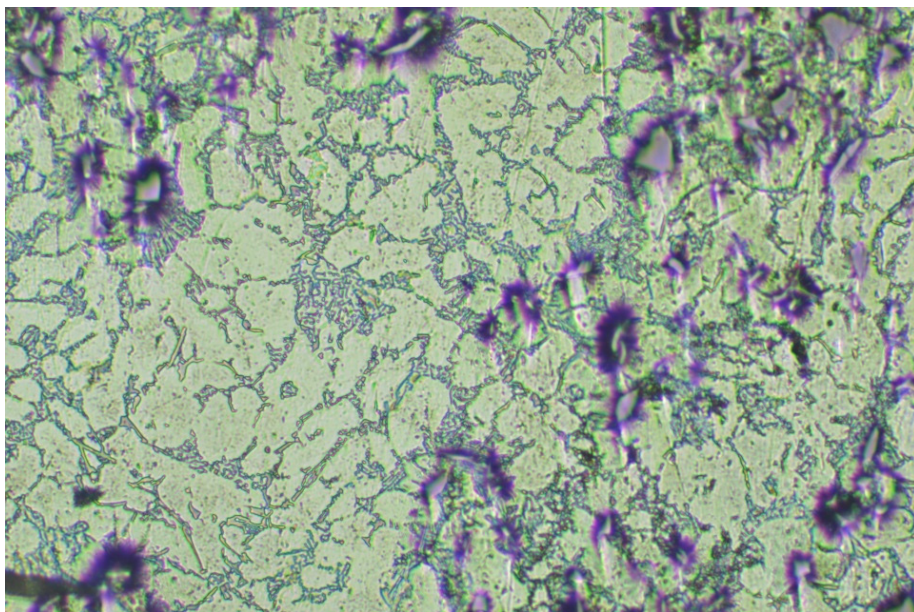


Figure 28; 200x.

4.2.3.4 Molds at 450 degrees

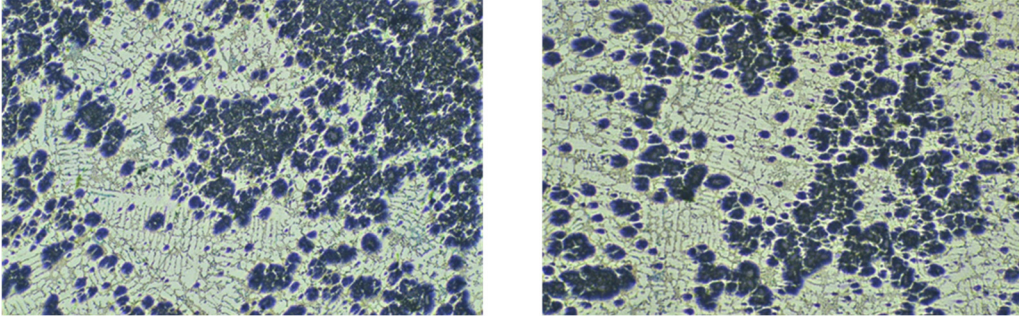


Figure 29; 50x.

Figure 29 shows the distribution and the quantity of silicon carbide particles. It is similar to the experiment with the mold temperatures set at 350 degrees.

Figure 30 shows the structure of the matrix. It is coarser than with cooler molds. The lighter areas are aluminium alloy, dendrites and eutectic precipitation. The darker lines are silicon in eutectic precipitate.

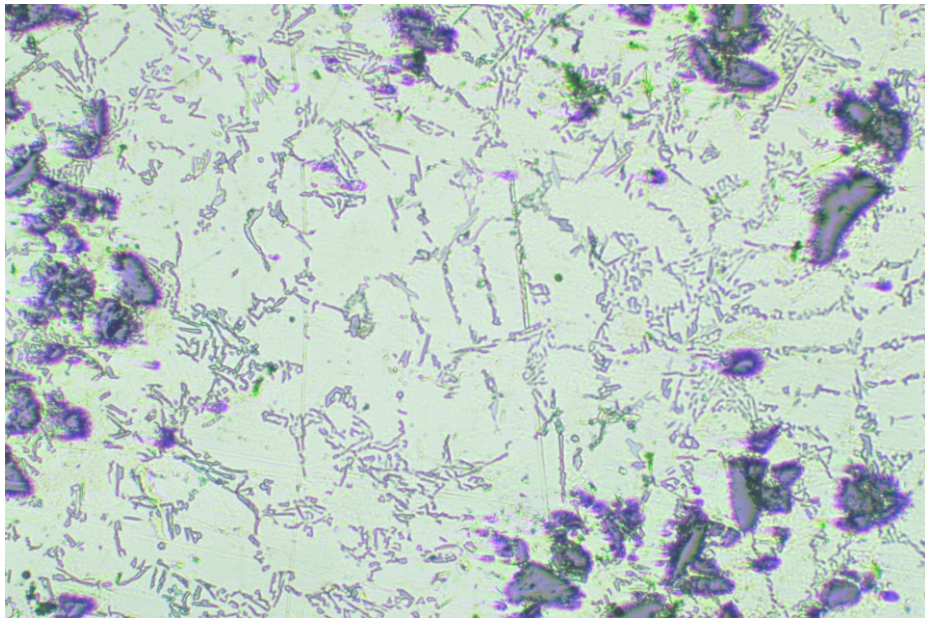


Figure 30; 200x.

4.2.3.5 *Molds at 750 degrees*

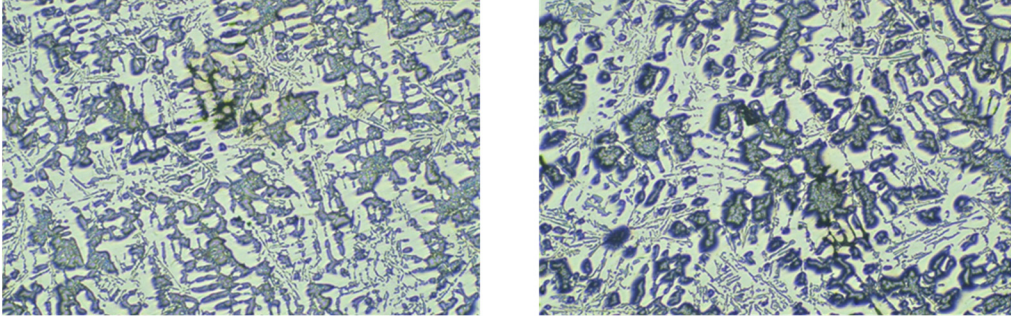


Figure 31; 50x.

When increasing the mold temperature to 750 degrees the structure became different from the other experiment with cooler molds. Figure 31 shows that the carbide content is much lower than before. Only a few SiC particles could be found in the entire sample.

The structure in Figure 32 looks as if the melt have been cooled slowly and give a long time to solidify.

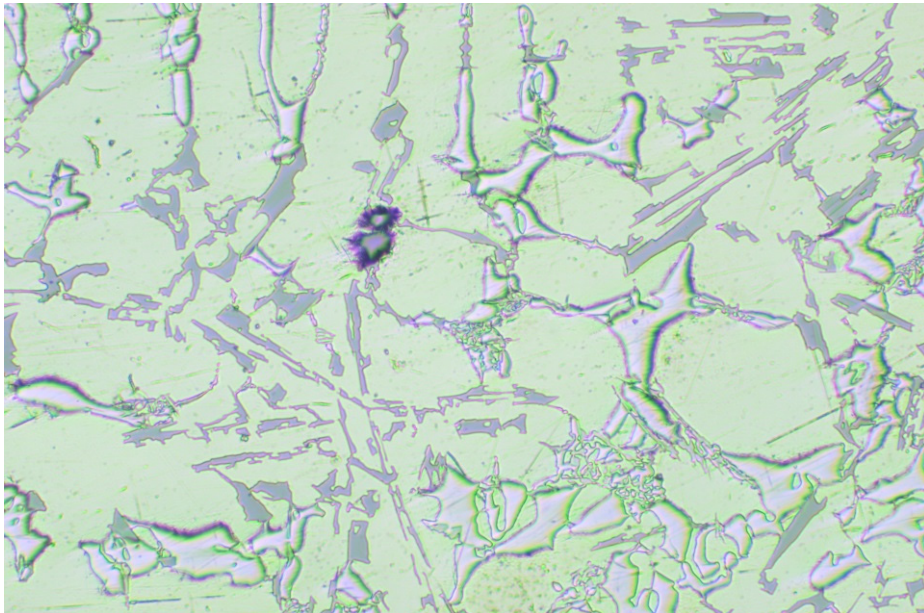


Figure 32; 200x.

4.2.4 SEM

Using a scanning electron microscope, areas with higher atomic density in solution with the matrix could be seen in all samples.

4.2.5 EDS

Especially the sample being cast at 750 degrees showed a larger amount of areas with higher atomic density; therefore the sample was examined using an energy dispersive spectroscopy. The EDS showed a lot of copper in solution with the matrix. It could also be seen that the silicon carbides had dissolved into the matrix since no particles could be found, but large amounts of silicon and carbon were found in solution with the matrix.

4.2.6 Carbide content

Table 9; Results of the carbide content analysis.

	% SiC [area]	% SiC [mass]	Average
RoomTemp	8,9	10,32	10,21
	8,7	10,09	
250°C	5,7	6,61	5,80
	5,4	6,26	
	4,5	5,22	
	4,4	5,10	
350°C	6,3	7,31	9,55
	15	17,40	
	3,4	3,94	
450°C	6,3	7,31	10,00
	9,3	10,79	
	12,7	14,73	
	6,2	7,19	

4.2.7 Hardness

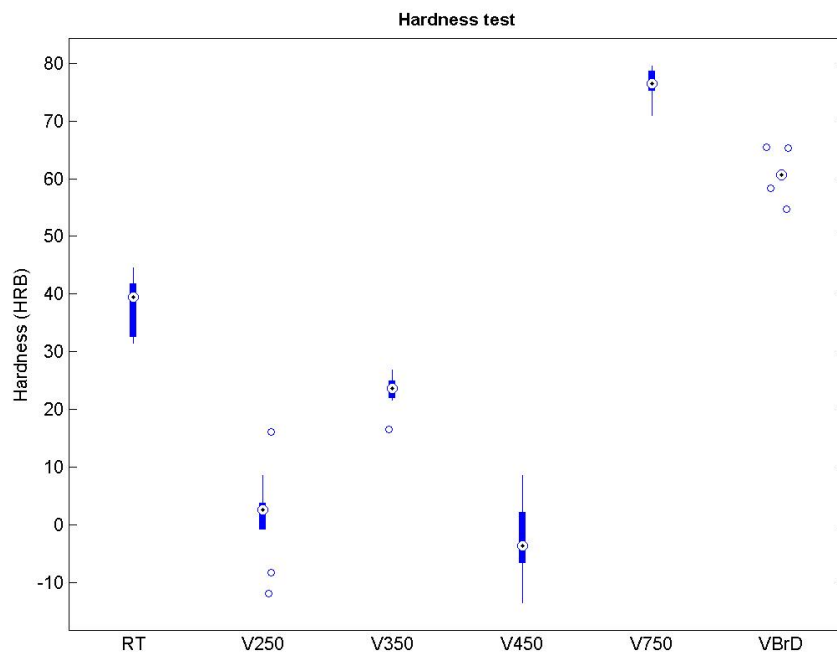


Figure 33; Hardness dependent on cooling rate.

The results from the hardness measurement can be seen in Figure 33. The results seem inconclusive; however there is a large scale trend of softer material with the higher mold temperatures. The main diversion is the sample at 750°C, which clearly is harder than the other samples tested.

4.2.8 Tensile test

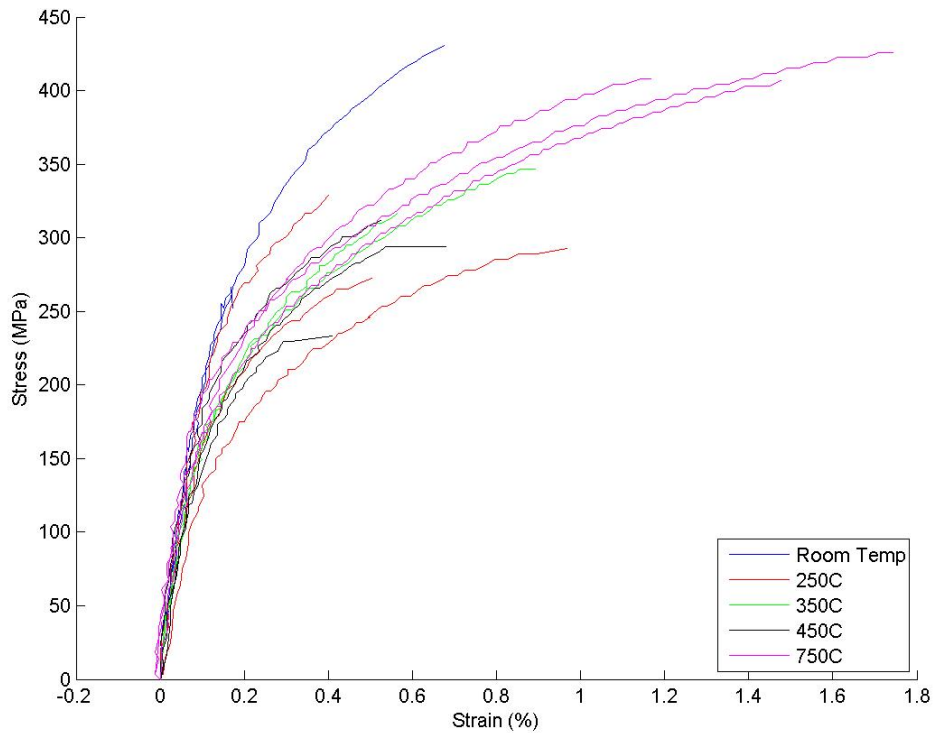


Figure 34; results from the tensile tests.

The results from the tensile tests can be seen in Figure 34. As can be seen, there is a tight grouping of the results from the 250°C, 350°C and the 450°C test with similar results. Room temperature stands out with a higher Young's modulus and overall a higher strength. The sample cast at 750°C shows a more ductile behavior with a much higher elongation at fracture. The large spread in data among samples cast at the same temperature is due to inclusions and porosities inherent to cast materials.

4.3 Part 2 - Silicon content

4.3.1 Comparison cooling rate

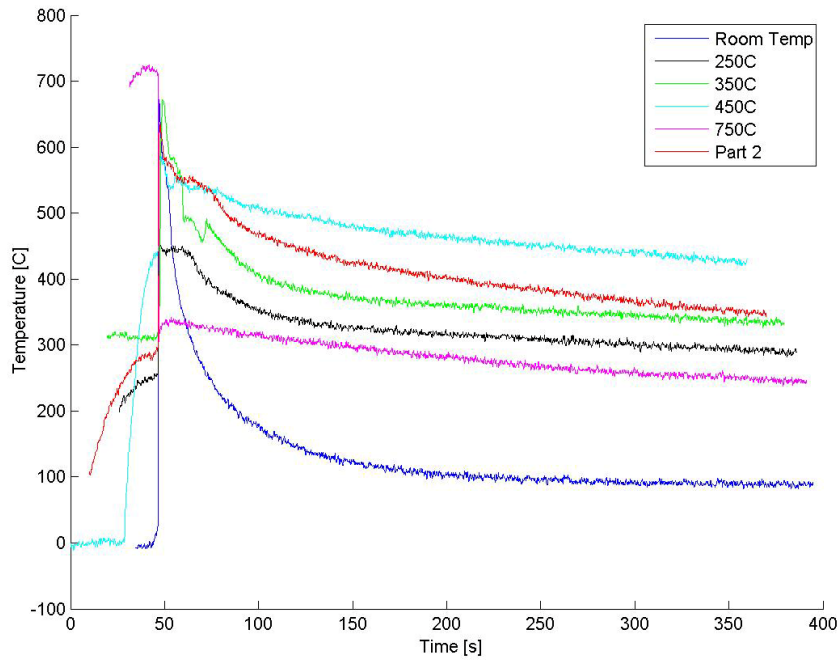


Figure 35; a comparison of the temperature curves from part 1 and part 2.

For the second part of the project, a thermocouple was inserted into the melt to make a comparison between the solidification times of the two parts. The cast alloy was identical to the one used by Volvo and in part one. At the time of casting the molds were 320 degrees.

4.3.2 Microstructure

4.3.2.1 9 percent silicon content

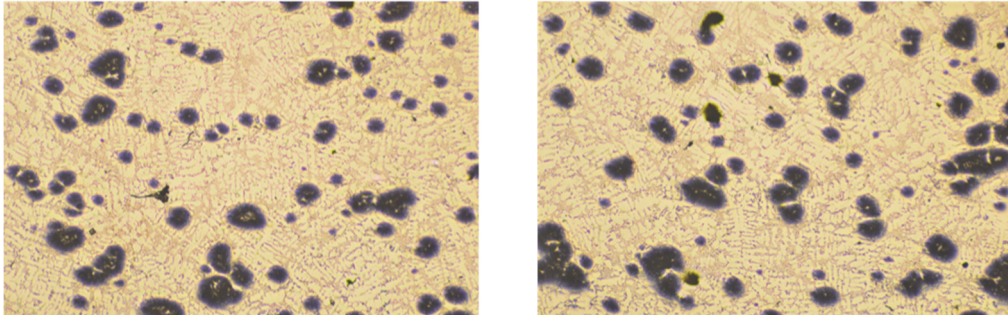


Figure 36; 50x.

All following experiments are performed with molds at 320 degrees.

Volvos brake disks contains 9 percent silicon today, therefore this is used as a reference. The distribution of silicon carbide particles can be seen in Figure 36. The distribution is quite poor with many particles clumped together.

The structure of the matrix can be seen in Figure 37 with fine dendrites.

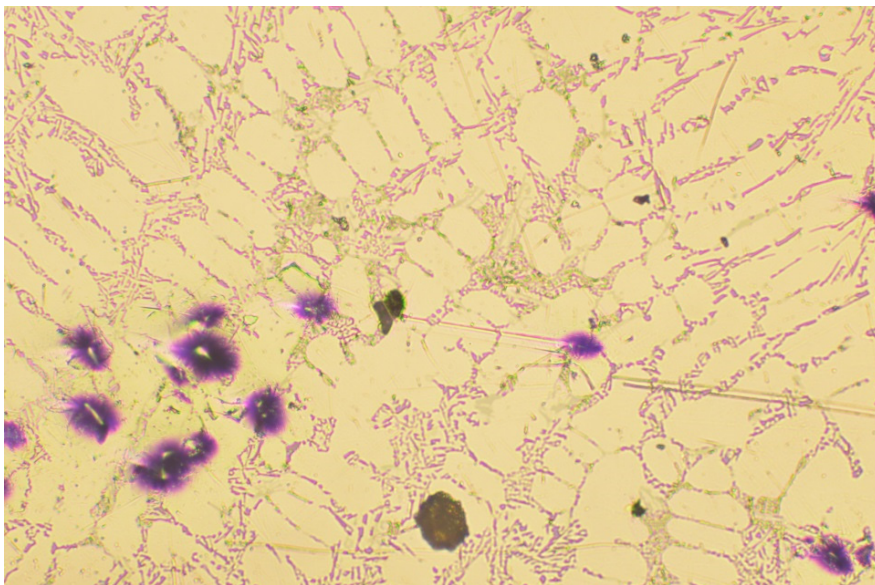


Figure 37; 200x.

4.3.2.2 7 percent silicon content

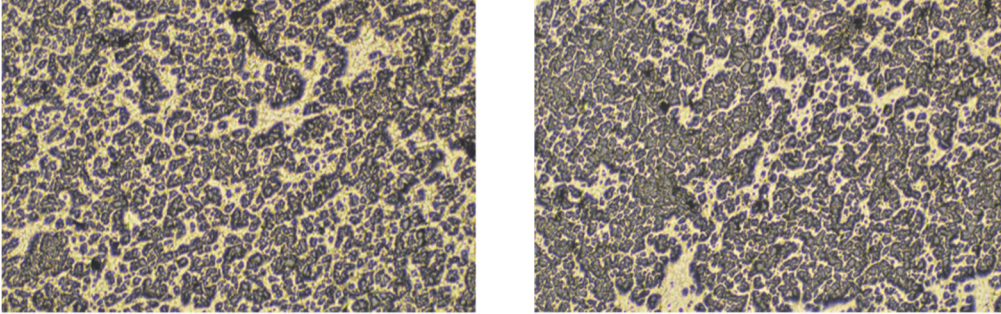


Figure 38; 50x.

To lower the silicon content to 7 percent more aluminium has been added to the melt.

The larger quantity of silicon carbide particles can be seen in Figure 38, and the distribution of particles is also better than the experiment with 9 percent silicon. Figure 39 shows the structure of the matrix.

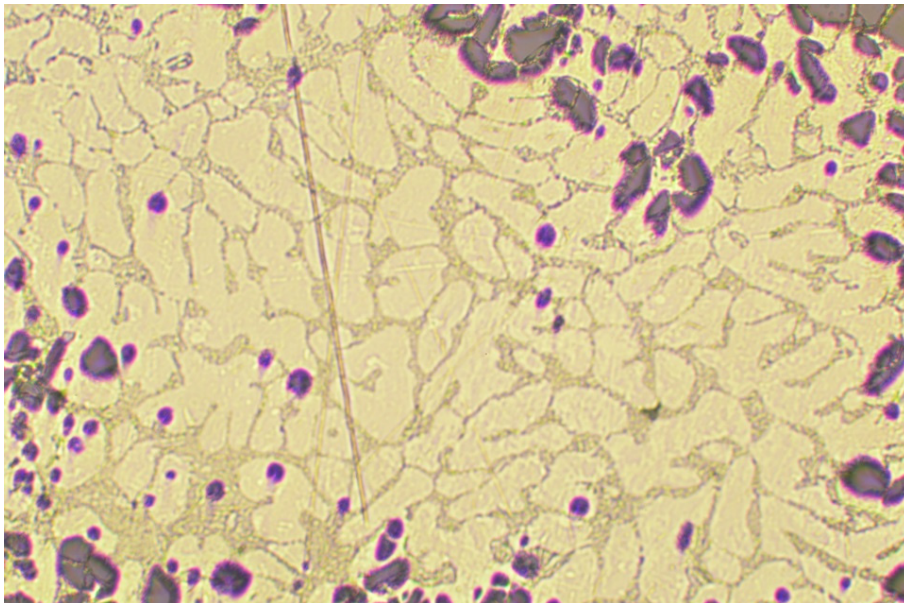


Figure 39; 200x.

4.3.2.3 11 percent silicon content

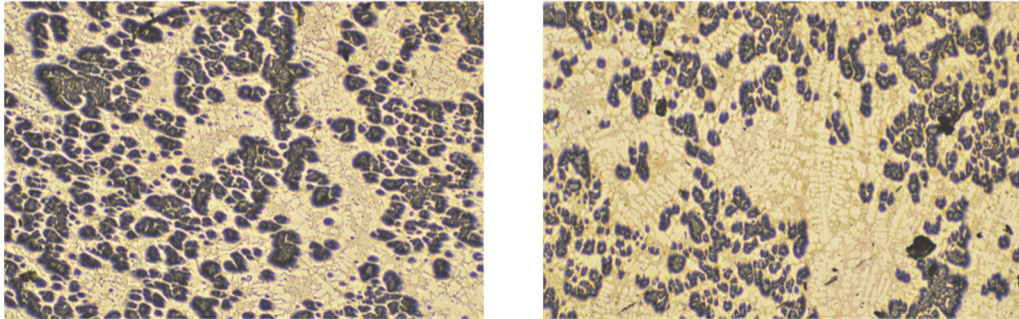


Figure 40; 50x.

To increase the silicon content pure silicon was added to the melt.

Figure 40 shows that the amount of carbides is lower than in the experiment with 7 percent silicon but more than in the experiment with 9 percent. The distribution of particles is inferior compared to the earlier experiments.

Figure 41 shows the matrix structure with large dendrites.

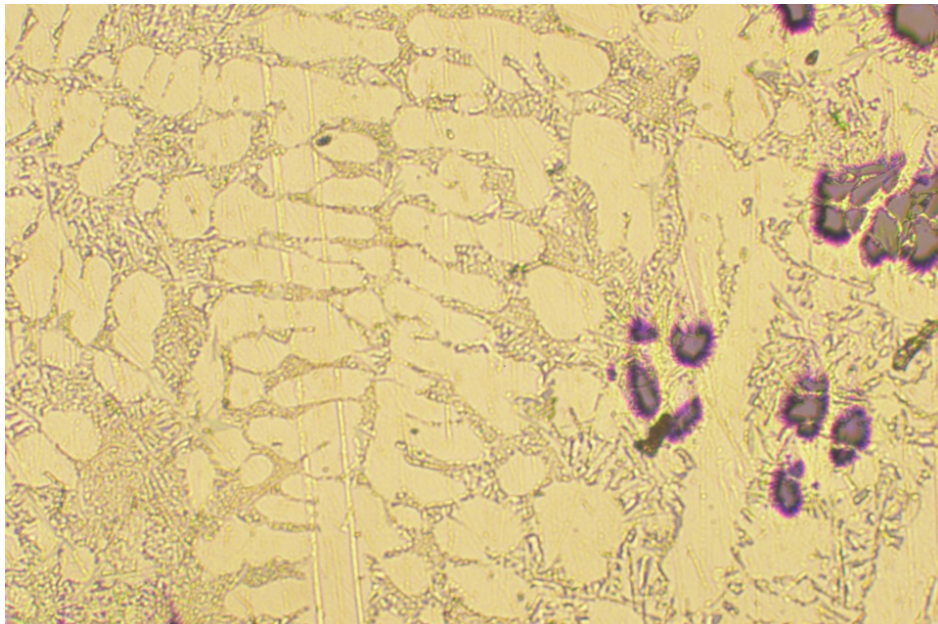


Figure 41; 200x.

4.3.2.4 12.5 percent silicon content

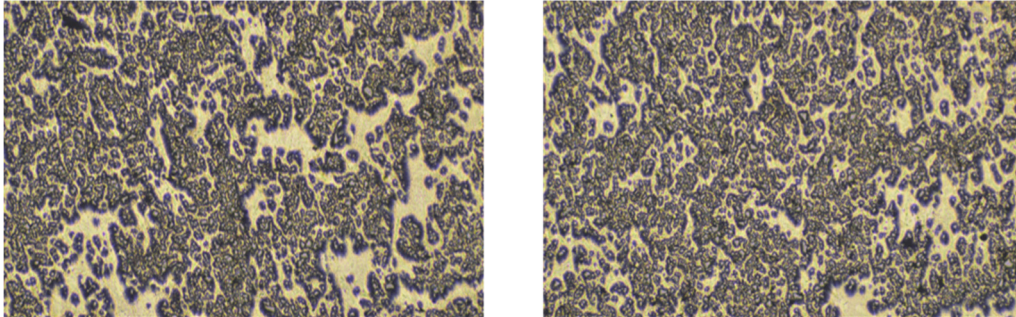


Figure 42; 50x.

To increase the silicon content further pure silicon was added to the melt. 12.5 weight percent silicon is the eutectic composition.

Figure 42 shows the distribution of SiC particles. The distribution and amount of particles are similar to the experiment with 7 percent silicon.

As can be seen in Figure 43, the matrix structure is coarser and has smaller dendrites.

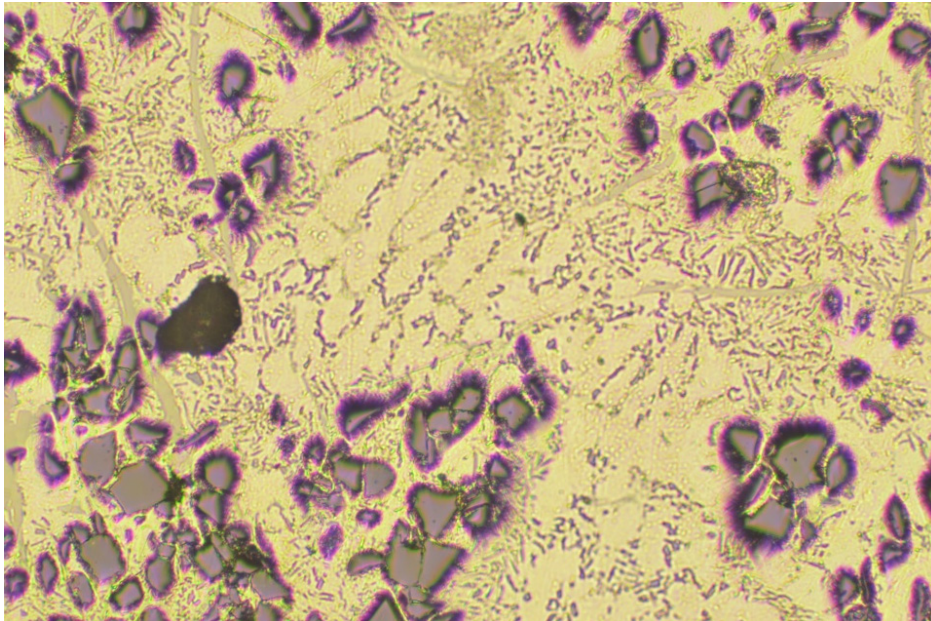


Figure 43; 200x.

4.3.3 Carbide content

Table 10; Analyze of carbide content in samples with varying silicon content.

	% SiC [area]	% SiC [mass]	Average
A	19,1	22,15	23,02
7 % Si	19,1	22,15	
	20,6	23,89	
	20,6	23,89	
Volvo	9,1	10,55	7,13
9 % Si	3,2	3,71	
B	6,8	7,89	10,73
11 % Si	11,7	13,57	
C	26,8	31,08	30,27
12.5 % Si	26,3	30,50	
	25,2	29,23	

4.3.4 Hardness

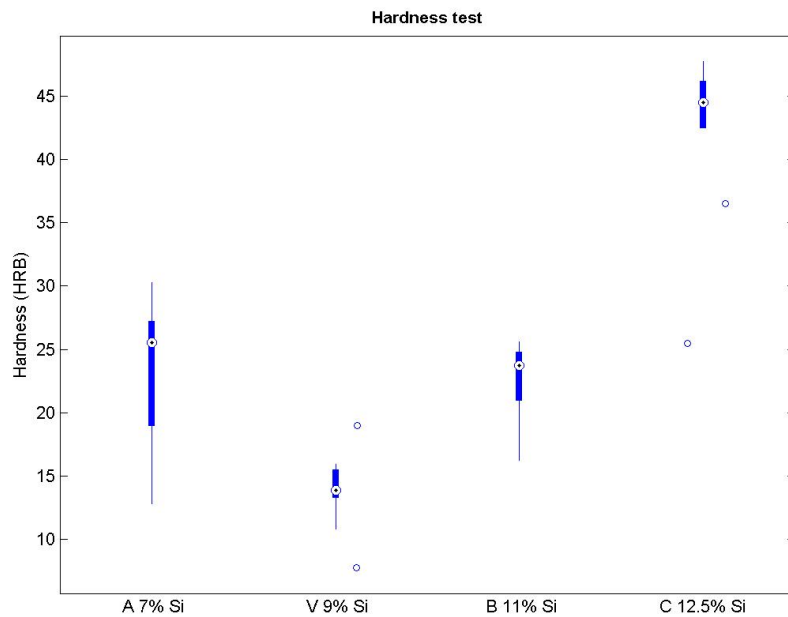


Figure 44; Hardness with varying matrix silicon content.

Figure 44 displays the results from the hardness measurements on the samples with varying silicon content in the matrix alloy. The general trend is harder material with higher silicon content, but the sample with seven percent silicon showed a larger spread, as well as a harder material than expected.

4.3.5 Tensile test

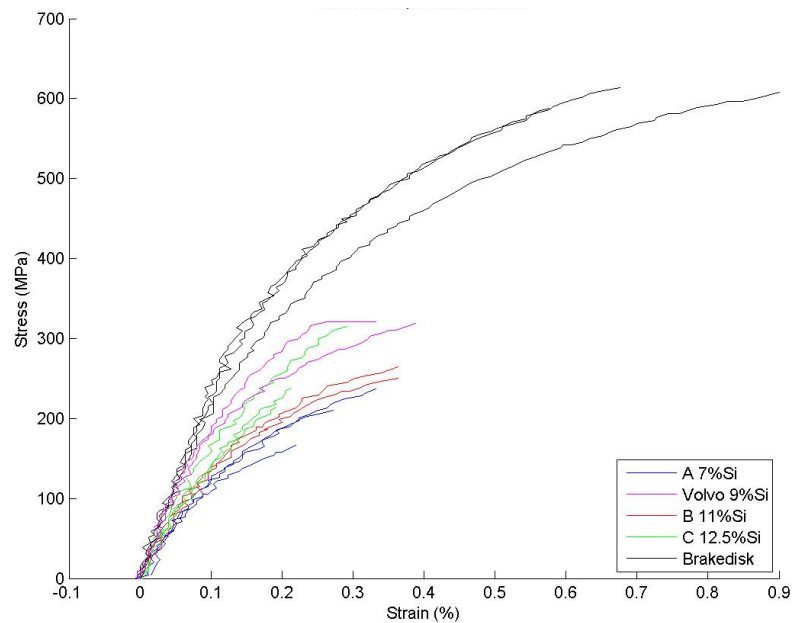


Figure 45; Result from the tensile tests of part two.

The results from the tensile tests can be seen in Figure 45, with the tests of machined brake disks added as a comparison. The result is partly supporting the theory with the higher silicon contents exhibiting a harder material with less elongation at fracture. The lowest of the 7% samples had large amounts inclusions, as can be seen in Figure 46. This might leave an explanation for the poor results of that particular rod.



Figure 46; A tensile testing rod with inclusions.

5 Conclusions

5.1 Discussion

Throughout the entire project we have had problems with the aluminium melt dissolving any metal it comes in contact with. For the copper molds this became apparent and later a problem as we gradually heated them to higher and higher temperatures. This led to larger forces required to force the cast rods from the molds and eventually we were unable to separate them from the molds.

In the beginning we were experimenting with both crucibles and paddles in austenitic stainless steel, as they in theory are inert up to 980 degrees. However in contact with liquid aluminium they quickly dissolved and formed intermetallic compounds. We also did tests with both titanium and Inconel to evaluate the possibilities to use these materials.

During the casting both molds were taken from the furnace at the same time, and then casting was done in one of them while the other waited in air. This procedure will lead to one of the molds having a slightly lower temperature at the moment of pouring. In the results from the temperature measurement, we can see that this fact does not seem to have any appreciable effect on the result.

As with all cast material, the samples produced in our experiment show a high degree of inclusions and porosities in the produced material. Naturally this can be seen in the cross section at fracture as this is where the stresses reach their maximum. Since all of the tested rods showed some sort of anomaly it should still leave us with consistent data and the conclusion that the results are comparable.

All stresses and elongations for the tensile tests have been calculated as engineering stresses and strain; that is force divided by original area and elongation divided by original length. As compared to true stress, force divided by actual area.

It is also clearly demonstrated the added effect of the squeeze casting technique, as the samples machined from factory produced brake disks shows almost double the tensile strength and a much higher ductility.

In the conversion from volumetric SiC content to mass percentages there is an inherent error, increasing with the deviation from the normal content of 21 wt%. This is because of the way the calculations are done, by comparing the actual area to the area of the ideal mixture and adjusting the mass content accordingly. This simplified calculation was chosen because of the speed and the accuracy at carbide content close to the baseline. The difficulty in the calculations arises due to the density of the alloy changing with increasing carbide content.

When we looked at the samples in the microscope, we could clearly see that the samples had been polished very hard. This leads to a great uncertainty in the analysis of the carbide content as the topography of the sample might create areas of shadow that could be interpreted as carbides. This would lead to an overestimate of the carbide content. Another factor to consider is that the hard polishing might reveal carbides in lower layers, again leading to an overestimate of the carbide content.

In the course of this project there has been some machining of the composite in question. Overall the machinability is fairly good; after all it is still based on aluminium. The main problem is in the wear of the tool, which under the wrong conditions can destroy a cemented carbide tool in a matter of seconds. With the correct cutting data we have even been able to drill in the material with a high-speed steel drill. The general recommendation is to use slow speeds and high feed. This leads to a protective build-up edge allowing the tools to function for long periods of time. For milling or turning with cemented carbide tools we used 60 meters/minute and 0.15 mm/revolution or 0.1 mm/tooth. For the machining of the tensile specimen, a diamond tool was used to ensure consistent results. For this we used 100 meters/min, the lower end of the recommended interval, but with the same feed and cuttingfluid.

5.1.1 Part 1 - Cooling rate

The results from the theoretical calculations are impressively close to the data measured later in the project. The success of the calculations must be attributed to the extremeness of the experiment, to cast 150 grams of aluminium in a solid 3,5 kg heated copper mold. Both materials have good thermal conductivity and therefore tend to eliminate any differences in temperature, which is supported by the very low Biot-number for the system.

The cast structure of the matrix shows a lot of dendrites. The dendrite structure becomes coarser when decreasing the cooling rate i.e increasing the mold temperature. With faster cooling there is an increase in nucleation sites, as dendrite growth starts at nucleation sites, there are more dendrites growing at the same time. When the dendrites have grown to a sufficient size they start interfering with each other and prevent further growth. This interference creates the finer structure.

Dendrites have a rounder shape in the experiment with molds at room temperature because the dendrites did not have time to grow prior to solidification. When increasing the mold temperature to 250 degrees, a more typical cast structure can be seen with a lot of fine dendrites. No distinct increase in dendrite size can be seen even if we increase the mold temperature further. In the experiment with molds at 350 degrees the dendrites are more randomly placed and one theory for this is that the dendrites have followed movements in the melt and then solidified.

With molds at 750 degrees the dendrites has grown very big and the structure is similar to one that if the sample has solidified slowly in the furnace. That is not surprising since the copper molds keeps temperature very well and the cooling occurs slowly. The large dendrites increase the ductility of the material and as can be seen in the tensile tests, the 750-sample has a larger plastic deformation prior to breakage.

When examining the 750 sample almost no carbide particles could be seen. A theory is that the silicon carbide has separated and formed carbon and silicon precipitates. That theory is supported by the examination in EDS, which showed large amounts of carbon and silicon in solid solution with the matrix. According to a study performed by J. C. Vialaet. al. in 1990 (23) silicon carbide began decomposing in aluminium alloy at 677 degrees. However they used a matrix alloy with only 0.5 % silicon and untreated silicon carbide. Volvo is using oxidized carbides, and we do not know what effect this has on the results.

Even in the sample at 250 degrees the amount of carbide particle is less than in the other. One theory is that segregation has taken place in the melt and that we therefore see less carbide particles in this particular sample. The only way to know for certainty is to polish more samples under the same conditions.

The hardness from the tested samples were at first a mystery, they did not match the theory. It all became clear when we saw the data plotted in Figure 33. In the figure the large scale trend can be seen, with material cast at lower temperatures showing a lower hardness. The biggest difference is the 750-sample, which is harder even than the brake disks produced by Volvo. One theory was that silicon from the carbides had dissolved into the alloy, changing it to hypereutectic alloy. An experiment performed by AnirudhBiswaset.al. at CMJ university support this theory as the hardness of our sample is close to the hardness of alloys with 16% silicon.(24) Another theory for the increased hardness of this sample is the high copper and carbon content of the matrix revealed by the examination in EDS.

When comparing the hardness test to the carbide content of the samples, we could see a connection between the two results. All samples except the 250°C have around 10 wt% SiC and fit in the theoretical trend between a slower cooling rate and a lower hardness. The sample cast at 250 degrees however only had around 6 wt% SiC, and is also softer than expected.

Tensile testing for our samples gave no conclusive results to the properties of the produced material. We can see a large uncertainty in the data with many of the samples showing similar properties overall. Looking at the large scale tendencies of the tests we see that materials cast in hotter molds show a more ductile behavior with a large elongation at the same stresses. The largest spread among a group of samples was with the 250°C samples.

The major difference between the different sample groups is for the samples cast at 750 degrees, which show the highest strength and the greatest elongation at breakage. The ductility of this material can be explained by the almost complete absence of carbides, as they instead dissolved into the matrix forming a hypereutectic alloy with greater strength.

5.1.2 Part 2 - Silicon content

Volvo's casting is done today with mold temperatures of 350 degrees, and we have therefore tried to replicate this temperature in our experiments.

At the start of part two of the project a quick test was done to determine the cooling rate for the steel molds. The alloy was identical to the one used in part one. Due to a static error in the oven temperature measurement the molds were actually 320°C, but as can be seen in the temperature curves in Figure 22 the result still closely resembles the cooling curve for the first part. The temperature curve, red line in Figure 22, shows a similar solidification time as the sample cast at 450 degrees but a recrystallization time more related to the sample cast at 350 degrees. This is because of the steel mold used in the experiment; with a lower thermal conductivity and a smaller mass than the copper molds used in part one, hence less energy to dissipate into the surrounding air.

The microstructure of the sample with 9 percent silicon has a cast structure with distinct dendrites with a clear boundary to the eutectic structure. With decreasing silicon content, α -phase is increasing. That can be seen as the dendrites are more compactly packed and the sample contains less eutectic structure. When increasing silicon content, i.e. decreasing α -phase, a reduced amount of dendrites can be seen and a more jagged edge between the different phases.

With increasing silicon content we can see a less than optimum distribution of the particles in the matrix. This is well coherent with theory as the particles are pushed by the solidifying eutectic structure to the grain boundaries. With increasing silicon there is an increase in the eutectic portion of the matrix leaving less room for the particles.

To lower the silicon content a more pure aluminium alloy was added to the melt to dilute the silicon. However the aluminium alloy used instead contained large amounts of magnesium, over 4 wt%. This could affect the overall results as even the small amount added would bring the magnesium content of the entire melt up to roughly 1%. Increasing amounts of magnesium in the melt increase the wettability of the liquid aluminium (25), this might change our results.

The hardness tests show a general trend to follow established theory, with higher silicon content showing a greater hardness. The main divergent from this is the samples with seven percent silicon. This sample shows the largest spread in sample data which can be explained by the porosity of the sample.

When comparing the sample's carbide content to the results from the hardness tests, we can see that 7 and 12,5 % silicon with higher carbide content also show a greater hardness than the other samples.

The results from the tensile tests can be seen in Figure 45, with the tests of machined brake disks added as a comparison. The result is supporting the theory with the higher silicon contents exhibiting a harder material with a lower elongation at fracture, however there is a peak in tensile strength for 9 % silicon. The lowest of the 7% samples had large amounts inclusions, as can be seen in Figure 46, which might leave an explanation for the poor results of that particular rod.

5.2 Sources of error

As in all projects of this magnitude there are multiple sources of error, the effects of which never can be fully estimated or compensated for. The single largest source of error must be the fact that we are researching cast samples, which inherently have a difficulty in controlling the produced material. Add to this various types of inclusion or gas pockets and effects of uneven cooling.

Particularly for part one it was difficult to control the time for the samples in the oven and the time used to agitate the melt, however the aim was always to keep it close to ten minutes.

The double melting of the higher temperatures might induce some sort of differences in the material structure as it was difficult to estimate the time needed to reheat the molds and place them in the furnace at the correct time. This uncertainty might lead to uneven results.

During the casting itself the greatest difficulties was in controlling the pouring time and to center the heated funnel in the molds to avoid contact with the walls.

As with all chemical experiments you must take the cleanliness of crucible and paddle in account. During the experiment we have observed a wear on the graphite paddle, which must mean that we have impurities either as particles or dissolved in the crystal structure. Also, because we are remelting brake disks we will get inclusion from the oxide layer in the melt.

The nitrogen gas used for the carbide transport was an ordinary commercial purity, which means it is allowed to contain minute amounts of oxygen. At these elevated temperatures, even the smallest amount will however be bound to the resulting material as aluminium oxide.

While discussing possible sources for error, there is always error in the measurement equipment. In our case, the regulators for the furnaces as well as the

thermocouples and their associated equipment. The thermocouples were calibrated at the beginning of the project with an accurate furnace, but all subsequent temperature measurements are highly dependent on the accuracy of this furnace.

Other sources for error might be the calibration of the hardness or tensile testing machines and the calibration of the extensometer

5.3 Summary

As this project comes to an end, we can draw some important conclusions. Overall the matrix alloy is behaving according to theory more or less disregarding the carbide particles, slower cooling rates and lower silicon contents produce a more ductile material.

We can only see a small difference between the cooling rates regarding the microstructure and the mechanical properties of the resultant material. A clear difference is only seen when the solidification time is taken to its extremes, with the samples cast in room tempered molds or molds heated to 750 degrees.

For the hardness there is a small difference between the samples, but only what would be expected from the theory. This leads to the conclusion that casting at 350 degrees produce a good material with good properties but the temperature is not critical.

While varying the silicon content we could clearly see the matrix behaving like theory. With increasing amounts of silicon we see decreasing amounts of dendrites and more lamellar structure.

The tensile testing shows a clear peak in tensile strength at 9 % silicon with higher silicon content showing a more brittle behavior and less strength.

Another conclusion we can draw from this project is the effect of the casting method. While investigating the effects of silicon content we tested two samples with the same alloy ingredients, one gravity cast for our experiments and one squeeze cast at Volvo. The sample produced by Volvo shows much better mechanical properties.

During our initial attempts to mix the ingredients we found that the mixing procedure is important for the result. There is probably more ways to achieve the same results, but we found no other ways of doing it successfully.

We know that the silicon carbide used by Volvo is oxidized prior to mixing, and we can see the positive effects as we have a minimum of dissolved particles.

5.4 Topics for future research

As metal matrix composites are a relative new field of study, there are many subjects that need more research. The following topics were initially part of this project but skipped due to time limitations or discovered during the scope of the project as possible topics for future research.

- Effectiveness of different wetting agents.
- Washed versus unwashed silicon carbide.
- Effects of different carbide contents.
- Effects of different particle sizes and size distributions.
- Temperature dependent strength.
- Investigate the effects of the electro plating on the mechanical properties.

6 References

1. **Ståhl, Jan-Eric and et. al.** *Properties and Processing of Aluminium Matrix Composites for Industrial Applications*. s.l. : VTT Manufacturing Technology, Espoo, Finland / Department of Production and Materials Engineering, LTH, Lund, Sweden, 1994. Vol. 3.
2. **Callister, William D. and Rethwisch, David G.** *Fundamentals of Materials Science and Engineering - An Integrated Approach*. 3:e. Hoboken : John Wiley & Sons Inc, 2008.
3. **Thyberg, Bertil and et. al.** *Gjuteriteknik*. Stockholm : Maskinaktiebolaget Karlebo, 1964. In Swedish.
4. **Kalpkjian, Serope and Schmid, Steven R.** *Manufacturing Engineering and Technology*. 6:e. Jurong : Ed. Prentice Hall, 2010.
5. **German, Randall M.** *Powder metallurgy & Particulate materials processing*. Princeton : Metal powder Industries Federation, 2005. pp. 50-62.
6. **Christian, J. W.** *The Theory of Transformations in Metals and Alloys*. Oxford : Pergamon Press, 1965.
7. **Ståhl, Jan-Eric and et. al.** *Gjutteknologi - Metalliska material*. Lund : Institutionen för Mekanisk Teknologi och Verktygsmaskiner, LTH, 1997. In Swedish.
8. **Iyengar, Srinivasan.** *Professor, Division of Materials Engineering, LTH*. [interv.] Emma Bengtsson and Mikael Hörndahl. Lund, June 19, 2013.
9. *Advanced Production Process and Properties of die cast magnesium Composites Based on AZ91D and SiC*. **Gertsberg, German, o.a., o.a.** 2009, Journal of Materials Engineering and Performance.
10. *Stiggjutning*. **Sjöberg, L.** Bokförlaget Bra Böcker AB, Höganäs : s.n., 1995, Nationalencyclopedia, Vol. 17.
11. **Ståhl, Jan-Eric and et. al.** *Metal Cutting*. Lund : Division of Production and Materials Engineering, LTH, 2012.
12. **Tyllered, G.** *Energitransport*. Lund : Institutionen för Mekanisk Värmeteori och strömningslära, LTH, 1984. In Swedish.
13. *OMEGA Temperature Measurement Handbook*. 7th. Bridgeport : Omega Engineering Inc., 2013. pp. z-21. Vol. MMXIV.
14. **Smallman, R. E. and Ngan, A. H. W.** *Physical Metallurgy and Advanced Materials*. 7th. Oxford : Elsevier Ltd., 2007.
15. *FEM Simulation and Experimental Validation of Cold Forging Behavior of LM6 Base Metal Matrix Composites*. **Joardar, Hillol, Sutradhar, Goutam och Sudar Das, Nitai.** Bhubaneswar, Orissa, India : u.n., 2012, Journal of Minerals and Materials Characterization and Engineering, Vol. 11.
16. *Investigation into Deformation Characteristics during Open-Die Forging of SiC Reinforced Aluminium Metal Matrix Composites*. **Verma, Deep, o.a., o.a.** Odisha, India : u.n., 2013, Journal of Powder technology.
17. *Effect of Forging Parameters on Low Cycle Fatigue Behaviour of Al/Basalt Short Fiber MMC*. **Karthigeyan, R. and Ranganth, G.** Tamil Nadu, India : s.n., 2013, The Scientific World Journal.
18. **Kaufman, John Gilbert and Rooy, Elwin L.** *Aluminum Alloy Castings*. s.l. : ASM International, 2004.
19. *HPDC of Advanced Reinforced Aluminium Alloys*. **Gofni, J., o.a., o.a.** 2004, La Metalurgia Italiana, Vol. 6.

-
20. **Rasmussen, N. W., Hansen, P. N. and Hansen, S. F.** High Pressure Die Casting of fibre-reinforced Aluminium by Preform Infiltration. [book auth.] G. Chadwick and L. Froyen. *Metal Matrix Composites*. Lyngby, Denmark : Elsevier Ltd, 1991.
21. **Martínez, H. Vladimir och Valencia, Marco F.** *Semisolid Processing of Al/B-SiC composites by Mechanical Stirring Casting and High Pressure Die Casting*. Institute of Energy, Materials and Environment. Medellín, Colombia : u.n., 2012.
22. *Effects of Porosity on Mechanical properties of MMC*. **Aqida, S. N., Ghazali, M. I. och Hashim, J.** Malaysia : u.n., 2004, Jurnal Teknologi.
23. *Stable and metastable phase equilibria in the chemical interaction between aluminium ad silicon carbide*. **Viala, J. C., Fortier, P. och Bouix, J.** Villeurbanne Cedex, France : u.n., 1990, Journal of Materials Science, Vol. 25.
24. *Mechanical Properties of Aluminium Alloy 22.92*. **Biswas, Anirudh och Bhalla, Deepak.** Shilong, Meghalaya, India : u.n., November 2012, Journal of Mechanical, Automobile and Production Engineering, Vol. 2.
25. *Optimum Parameter for Wetting Silicon Carbide Aluminium Alloys*. **Pech-Canul, M. I., Katz, R. N. and Makhlof, M. M.** 2, 2000, journal of Metallurgical and Materials Transactions, Vol. 31, pp. 565-573.

Images

All images, unless otherwise stated, is copyrighted to the authors.

Figure 1; Aluminium – Silicon phase diagram, taken from Globalsino.com

<http://www.globalsino.com/micro/1/1micro9989.html>

Figure 2; Used under creative commons, originally created by Wikipedia user Wizard191.

Adapted by the authors.

http://upload.wikimedia.org/wikipedia/commons/e/e1/Cooling_curve_alloy.svg

Figure 3; Used under creative commons, created by Wikipedia user Wizard191

http://upload.wikimedia.org/wikipedia/commons/b/b4/Cooling_curve_pure_metal.svg